A&A 369, 889–907 (2001)
DOI: 10.1051/0004-6361:20010101

Astronomy & Astrophysics

A study of polarized spectra of magnetic CP stars: Predicted vs. observed Stokes IQUV profiles for β CrB and 53 Cam⋆

S. Bagnulo[1,⋆⋆], G. A. Wade[2,⋆⋆⋆], J.-F. Donati[3], J. D. Landstreet[4], F. Leone[5], D. N. Monin[6], and M. J. Stift[1]

[1] Institut für Astronomie, Universität Wien, Türkenschanzstrasse 17, 1180 Wien, Austria
e-mail: bagnulo@astro.univie.ac.at & stift@fedelma.astro.univie.ac.at
[2] Astronomy Department, University of Toronto at Missisauga, L5L 1CS Ontario, Canada
[3] Observatoire Midi-Pyrénées, 14 avenue Édouard Belin, 31400 Toulouse, France
e-mail: donati@obs-mip.fr
[4] Physics & Astronomy Department, The University of Western Ontario, London, N6A 3K7 Ontario, Canada
e-mail: jlandstr@astro.uwo.ca
[5] Osservatorio Astrofisico di Catania, Città Universitaria, 95125 Catania, Italy
e-mail: fleone@ct.astro.it
[6] Special Astrophysical Observatory of the Russian AS, Nizhnij Arkhyz 357147, Russia
e-mail: mosha@sao.ru

Received 20 September 2000 / Accepted 12 January 2001

Abstract. We present a comparison of observed and calculated Stokes $IQUV$ spectra of two well-known magnetic chemically peculiar stars, β Coronae Borealis and 53 Camelopardalis. The observed Stokes spectra were recently described by Wade et al. (2000a), and have been complemented with additional circularly polarized spectra obtained at the Special Astrophysical Observatory. The calculated spectra represent the predictions of new and previously published magnetic field models derived from the analysis of some surface averaged field estimates (e.g., longitudinal field, magnetic field modulus, etc.). We find that these magnetic models are not sufficient to account fully for the observed Stokes profiles – particularly remarkable is the disagreement between the predicted and observed Stokes Q and U profiles of 53 Cam. We suggest that this should be interpreted in terms of magnetic morphologies which are significantly more complex than the second-order multipolar expansions assumed in the models. However, it is clear that some of our inability to reproduce the detailed shapes of the Stokes $IQUV$ profiles is unrelated to the magnetic models. For many metallic ions, for both stars, we found it impossible to account for the strengths and shapes of the observed spectral line profiles when we adopted a unique value for the individual ion abundance. We suggest that this results from strongly non-uniform distributions of these ions as a function of optical depth (i.e., chemical stratification), a hypothesis that is supported by comparison with simple chemically stratified models.

Key words. stars: magnetic fields – polarization – stars: chemically peculiar – stars: individual: β CrB – stars: individual: 53 Cam

1. Introduction

The spectra of magnetic chemically peculiar (CP) stars of upper main sequence are exceedingly complex, and their modelling represents an extraordinary challenge for stellar astronomers. Magnetic CP stars are characterised by remarkably rich line spectra, often containing numerous unidentified features. Compared to the solar case, overabundances up to a few dex are often inferred for some iron peak and rare earth elements, whereas some other chemical elements are found to be underabundant. Some of the more slowly rotating stars ($v_{\rm e} \sin i \lesssim 5\,{\rm km\,s^{-1}}$) display lines which are split into multiple components because of the Zeeman effect. In faster rotators, Zeeman splitting is usually washed out by rotational Doppler broadening; yet, magnetic intensification can strongly affect shape and strength of spectral lines. In polarized light, spectral lines exhibit complex features, both in circular

Send offprint requests to: S. Bagnulo

⋆ Based on observations obtained with the 2 m Bernard Lyot telescope of the Pic-du-Midi Observatory, the 1 m telescope of the Special Astrophysical Observatory, and the 0.9 m telescope of the Osservatorio Astrofisico di Catania.

⋆⋆ *Present address:* European Southern Observatory, Casilla 19001, Santiago 19, Chile; e-mail: sbagnulo@eso.org
⋆⋆⋆ *Present address:* Dépt. de Physique, Université de Montréal, C.P. 6128 succ Centre-Ville, Montréal, QC, Canada H3C 3J7; e-mail: wade@astro.umontreal.ca

polarization (Stokes V) and linear polarization (Stokes Q and U) – the latter often at the limit of detection of the best currently available instrumentation. Shape and strength of Stokes profiles, together with stellar luminosity, change periodically with time, typically on a timescale of a few days, although it is not unusual to observe a periodicity of several years, or tens of years.

The period of the variability of the photometry and of the spectral features is firmly associated with the stellar rotation period, and our interpretation of the periodic variability of the observed phenomena is rooted in the *Oblique Rotator Model* (ORM; Stibbs 1950). The ORM holds that the atmospheres of CP stars are permeated by strong magnetic fields, ranging in strength from a few hundred G to a few ten thousand G, organised on a large-scale. Abundances of some (but not all) chemical elements are distributed in a nonuniform fashion throughout the photosphere (and hence over the stellar "surface"). The magnetic field and the abundance distributions are "frozen" into the star, and are generally *not* distributed symmetrically about the stellar rotation axis. Therefore, as the star rotates, different aspects of the chemical abundance and magnetic field distributions are presented to the observer, resulting in the observed line strength, shape and polarization variability.

It is generally agreed that the formation of the chemical nonuniformities of CP stars, and more generally the peculiar chemical abundances implied by the rich line spectra, results from various chemical transport mechanisms operating in their magnetically-stabilised radiative photospheres. The key process is *microscopic chemical diffusion*: competition between gravitational settling and radiative levitation is believed to result in the selective diffusion of various trace elements into (or out of) the line-forming region (Michaud 1970). The peculiar abundances of CP stars directly reflect the resultant accumulation or depletion of these elements. Chemical nonuniformities are believed to result from the additional influence of the magnetic field on the diffusing ions, possibly in combination with the influence of a weak, magnetically-directed wind (e.g., Babel 1992). The magnetic field is itself probably a fossil remnant, either of a field swept up by the star during formation, or possibly generated during pre-main sequence evolution (e.g., Moss 1994). The magnetic field might also be responsible for angular momentum loss (most likely occurring during the pre-main sequence phase), as one finds that magnetic CP stars are much slower rotators than non chemically peculiar stars of similar spectral type (see Stępień 2000 for a recent study of this phenomenon). Our ability to confront and direct such theoretical investigations relies heavily on our ability to infer the topology of the magnetic field of CP stars and the distribution of chemical elements in their photospheres, hence on our ability to reproduce the observed spectra.

The *Zeeman Doppler Imaging* (ZDI) or *Magnetic Doppler Imaging* (MDI) (Semel 1989) – based on an inversion of Stokes profiles subject to a regularising constraint (such as maximum entropy) – is a promising tool for the modelling of stellar magnetic fields, in particular when applied to objects characterised by fairly complex field topologies such as late-type stars, and to relatively fast rotators (Brown et al. 1991; Donati & Brown 1997; Donati et al. 1999a). However, these techniques have not yet been applied systematically to stars with magnetic morphologies organised on a large scale (such as CP stars), and Donati (2001) suggests that Stokes $IQUV$ profile time-series do not contain enough information to reconstruct organised magnetic fields, without a prior assumption about the field topology. So it makes sense to explore alternative methods which can complement or in certain cases even substitute for ZDI.

An alternative approach involves the recovery of the magnetic field topology *prior* attempting to model the spectra. The magnetic field topology is inferred through the interpretation of some surface averaged magnetic field estimates, hereafter referred to as *magnetic observables*, which can readily be obtained even from (relatively) low-resolution, low S/N spectra, without solving the problem of the radiative transfer. These observables strongly reflect the characteristics of the magnetic field, and are only weakly affected by chemical nonuniformities (Mathys 1999). For a long time, the *mean longitudinal magnetic field* $\langle \mathcal{B}_z \rangle$ has been the main quantity derived either from Stokes I and V observations of metallic absorption line profiles – mostly iron peak elements (Babcock 1947; Mathys 1991) – or from photopolarimetric measurements in the wings of the Hβ Balmer line (Borra & Landstreet 1973, 1980). More sophisticated techniques can extract additional magnetic observables from Stokes I and V profiles of metallic lines, allowing one the determination the *mean magnetic field modulus* $\langle \mathcal{B} \rangle$ (Babcock 1960a; Mathys et al. 1997), the *crossover* $v_{\rm e} \sin i \, \langle {\rm d}\mathcal{B}_z \rangle$ (Mathys 1995a), and the *mean quadratic magnetic field* $\langle \mathcal{B}^2 + \mathcal{B}_z^2 \rangle^{1/2}$ (Mathys 1995b). The analysis of Stokes Q and U profiles provides useful constraints on the transverse components of the magnetic field (Mathys 1999); so can linear polarimetric observations obtained through a broadband filter (Landolfi et al. 1993). In fact, since noise often hampers the detection of Stokes Q and U signatures in line profiles, measurements of broadband linear polarization (BBLP) may even be preferable to spectropolarimetry (e.g., Leroy et al. 1996). So far, most modelling techniques for magnetic fields of CP stars have been based on the combined interpretation of these magnetic observables (see Bagnulo et al. 2000 and Landstreet & Mathys 2000, for the most recent works). It is assumed that the magnetic field can be represented by a low-order multipolar expansion, and its topology is recovered by means of an inversion algorithm applied to the *magnetic curves*, i.e., the magnetic observables as functions of rotational phase.

Although we are still incapable of using Stokes $IQUV$ spectra for a simultaneous recovery of the magnetic topology and element distribution in the photospheres of CP stars, we can combine the diagnostic content of the magnetic observables with a direct comparison of Stokes profiles, i.e., first we derive a tentative model for the

magnetic field by means of a least-square inversion technique applied to the magnetic observables, and we subsequently compute synthetic Stokes profiles for these tentative magnetic models, in order to compare them to the observations. This can show whether the models are realistic representations of the true stellar magnetic topologies, and reveal relationships between magnetic topology and element distribution. In this paper we present this kind of investigation for two well known CP stars: β Coronae Borealis and 53 Camelopardalis.

2. Targets and scope of the investigation

Attempting to reproduce time series of polarized spectra of magnetic CP stars is a task which requires dense coverage in rotational phase and good S/N in all Stokes components; β CrB and 53 Cam are stars for which suitable data sets have recently become available.

The modelling of the magnetic observables of β CrB is quite challenging. Taken together, the respective shapes of the curves of longitudinal field and mean field modulus are inconsistent with an axisymmetric morphology as the extrema of the field modulus variations are not in phase with the extrema of the longitudinal field variations (e.g., Stift 1975). The star furthermore turns out to have an unfavourable orientation, with its rotation axis almost parallel to the line of sight. This implies that little more than half of the stellar surface becomes visible to the observer during a full rotational cycle. The inverse problem becomes particularly ill-conditioned and one can expect to encounter multiple solutions (Landolfi et al. 1998). Bagnulo et al. (2000) gave a combined interpretation of all the magnetic curves of β CrB assuming a magnetic morphology characterised by a second order, non-axisymmetric multipolar expansion (i.e., a dipole plus a quadrupole arbitrarily oriented), finding indeed two different models that could equally well explain the magnetic curves. Wade et al. (2000a) obtained a superb series of Stokes $IQUV$ spectra of β CrB, fully sampling the rotational cycle. An examination of these spectra reveals that numerous individual spectral lines exhibit clear Stokes Q and U signatures. The existence of previously published models of the magnetic field of β CrB, combined with the high quality of the spectropolarimetric observations, makes β CrB an excellent target for this investigation.

The pioneering investigation of 53 Cam by Landstreet (1988) led to an axisymmetric magnetic field model characterised by the superposition of a dipole, a linear quadrupole and octupole, all aligned with the dipole. This model predicts prominent Zeeman signatures in the Stokes Q and U profiles (Wade et al. 2000a), frequently attaining full amplitudes as large as 5–10% of the continuum flux. However, a series of Stokes $IQUV$ spectra of 53 Cam obtained by Wade et al. (2000a) are at gross variance with these expectations, the observed linear polarization signatures being substantially weaker than predicted. Because of the failure of Landstreet's (1988) model to reproduce the linear polarization signatures of 53 Cam, we will attempt to develop a more satisfactory model of the magnetic field of 53 Cam, based on the inversion method described by Bagnulo et al. (2000). Synthetic spectra based on the resulting model will be compared with both the spectropolarimetric observations obtained by Wade et al. (2000a), as well as with additional Stokes I and V observations obtained at the 1 m telescope of the Special Astrophysical Observatory (SAO).

Historically, very little effort has been directed at performing comparison of synthetic Stokes profiles of magnetic CP stars with spectropolarimetric observations; the few exceptions are the works by Landstreet (1988), Landstreet et al. (1989), Donati et al. (1990), Stift & Goossens (1991), and Wade et al. (2000a). From our perspective, there are three primary reasons for this.

i) Until very recently, no high-resolution, high signal-to-noise ratio spectropolarimetric observations were available. In particular, over an inordinately long time, the Stokes Q and U profiles of β CrB obtained by Borra & Vaughan (1977) were the only ones available for any CP star.

ii) On the whole, comparatively little attention has been paid by stellar astronomers to spectral line synthesis in magnetic atmospheres. This appears somehow surprising, as modelling Stokes profiles observed e.g. in sunspots or in the network has become "routine" work for solar physicists. We attribute this to the fact that the synthesis of spectral lines in magnetic stellar atmospheres is very expensive computationally, e.g., it must be performed over a 2-D grid, not just at a single point. Furthermore, the fact that we observe only disk-integrated light from other stars means that inversion of the observations is much more ill-conditioned than in the solar case.

iii) Although organised on a large scale, the magnetic topologies of CP stars cannot always be successfully explained by dipolar or even multipolar axisymmetric fields. It has repeatedly proven difficult, if not impossible, to recover models capable of correctly predicting all of the magnetic observables, even more so to account for the shape of the observed Stokes profiles.

Thanks to impressive advances in instrumentation, hardware and software, the situation has improved radically over the last few years. The scope of our work can now be more ambitious than in the past: as a direct result of the development of the relevant instrumentation and observing protocols (Semel et al. 1993; Donati et al. 1997 and Donati et al. 1999b), we have high-quality observations of Stokes $IQUV$ profiles for a selection of magnetic stars at our disposal (Wade et al. 2000a). As well, thanks to the development of fast processors and the ability to run calculations in parallel we are able to rapidly synthesise Stokes profiles for CP stars over large spectral intervals (see Wade et al., in preparation, for a review and comparison of three different codes for polarized radiative transfer in atmospheres permeated by strong magnetic fields). We feel that these new observations and computational tools, in combination with an increasingly sophisticated framework describing the magnetic topology (see

Bagnulo et al. 1996) makes a meaningful comparison of synthetic and observed Stokes spectra finally possible. Admittedly, the present work is lacking a quantitative description of the effects of element abundance inhomogeneities, since for the computation of synthetic Stokes profiles, a homogeneous distribution of all chemical elements over the stellar surface has been assumed throughout. A qualitative discussion of the geographic distribution of the chemical elements at the surface of the stars is given in Sect. 7.

3. Spectropolarimetric observations

3.1. Observations at Pic-du-Midi

Stokes $IQUV$ spectra of β CrB and 53 Cam were obtained using the MuSiCoS cross-dispersed échelle spectrograph (Baudrand & Böhm 1992), coupled via a dual optical fibre to a dedicated polarimetric module (Donati et al. 1999b) which was mounted at the $f/25$ Cassegrain focus of the 2 m Bernard Lyot Telescope (TBL) at Pic-du-Midi Observatory. All spectra were obtained with a spectral resolution of $R = 35\,000$. Observations of β CrB at 17 rotational phases were taken during 1997–1999 with a typical exposure duration of 1200 s per Stokes parameter and a typical S/N of about 600:1 or 700:1 (for a 4.5 km s^{-1} bin). Observations of 53 Cam at ten rotational phases were obtained during 1997–1998 with a typical exposure duration of 2400 sec and a typical S/N of 150:1 or 200:1. The observations are described in detail by Wade et al. (2000a), and an example of a complete reduced Stokes $IQUV$ spectrum of β CrB is provided by Wade et al. (2000b).

3.2. Observations at SAO

We obtained Stokes I and V spectra of 53 Cam at six rotation phases during the nights of March 6–8 1999, April 3 1999 and April 6–7 1999 with the coudé échelle grating spectrograph CEGS attached to the 1 m telescope at the Special Astrophysical Observatory, Russia. With a 2″ entrance slit, the instrument configuration (Musaev 1996) yields a resolving power of about 40 000 over a spectral range from 4000 to 8000 Å. The typical S/N achieved was $\gtrsim$100.

3.3. Observations at the Osservatorio Astrofisico di Catania

The fibre-fed REOSC spectrograph of the 0.9 m telescope of the *Osservatorio Astrofisico di Catania*, equipped with the polarimetric module, was used to obtain low resolution Stokes I and V spectra ($R = 16\,000$) of 53 Cam at three rotational phases, with $S/N \gtrsim 100$. The equipment, observations and data reduction procedures are described by Leone et al. (2000). A detailed log of these observations is given by Leone & Catanzaro (2001). Due to the low resolution, this data set was not used for a direct comparison of synthetic vs. observed spectra, but only for determinations of longitudinal field (see Sect. 3.4 below).

Table 1. Determinations of the mean longitudinal magnetic field of 53 Cam. The rotation phase, given in Col. 2, is defined according to the ephemeris of Hill et al. (1998), i.e., JD = 2448498.186 + (8.02681 ± 0.00004) E

HJD −2450000	Rotation Phase	$\langle \mathcal{B}_z \rangle$ (G)	$\sigma_{\langle \mathcal{B}_z \rangle}$ (G)	Spectra
1244.443	0.136	2700	300	SAO
1245.207	0.231	3400	270	SAO
1246.230	0.358	2970	430	SAO
1262.369	0.369	3130	450	Catania
1264.376	0.619	−3335	470	Catania
1265.325	0.737	−4570	560	Catania
1272.328	0.610	−2960	275	SAO
1275.274	0.977	−800	500	SAO
1276.254	0.108	2510	270	SAO

3.4. New determinations of longitudinal field for 53 Cam

From the SAO and Catania spectra we obtained nine measurements of the longitudinal magnetic field, following the procedure described by Leone et al. (2000). The measurements are listed in Table 1. Measurements of the longitudinal field of 53 Cam from the Pic-du-Midi spectra were reported by Wade et al. (2000c).

3.5. Comparison of the polarized spectra

Inspection to Table 2 of Wade et al. (2000c) and Table 1 of this paper shows full consistency among the longitudinal field determinations obtained from the Pic-du-Midi, SAO and Catania spectra (see also Fig. 7 in Sect. 6.1.1). The detailed features of the observed Stokes profiles are another matter, and these depend strongly on the magnetic configuration presented to the observer. Accordingly, a comparison between the Stokes profiles as obtained using the different instruments would be meaningful only for spectra acquired at identical rotation phases. Although we have no Pic-du-Midi and SAO spectra obtained at identical rotation phases, we can still make such a comparison with the assistance of numerical simulations. The left panels of Fig. 1 show Stokes I and V spectra obtained at Pic-du-Midi at JD = 2450496.449 and JD = 2450497.315 (phase = 0.95 and 0.06, respectively, according to the ephemeris of Hill et al. 1998), compared with those obtained at SAO at JD = 2451275.274 (phase = 0.98). There are clear differences among all three spectra in both Stokes I and Stokes V. How much of these differences can be ascribed to rotational variability of the spectrum of 53 Cam (as all three spectra were obtained at slightly different rotation phases), and how much is due to the use of the different instrumentation and data processing, and hence different systematics, spectral resolutions and signal-to-noise ratios? To attempt to evaluate the relative

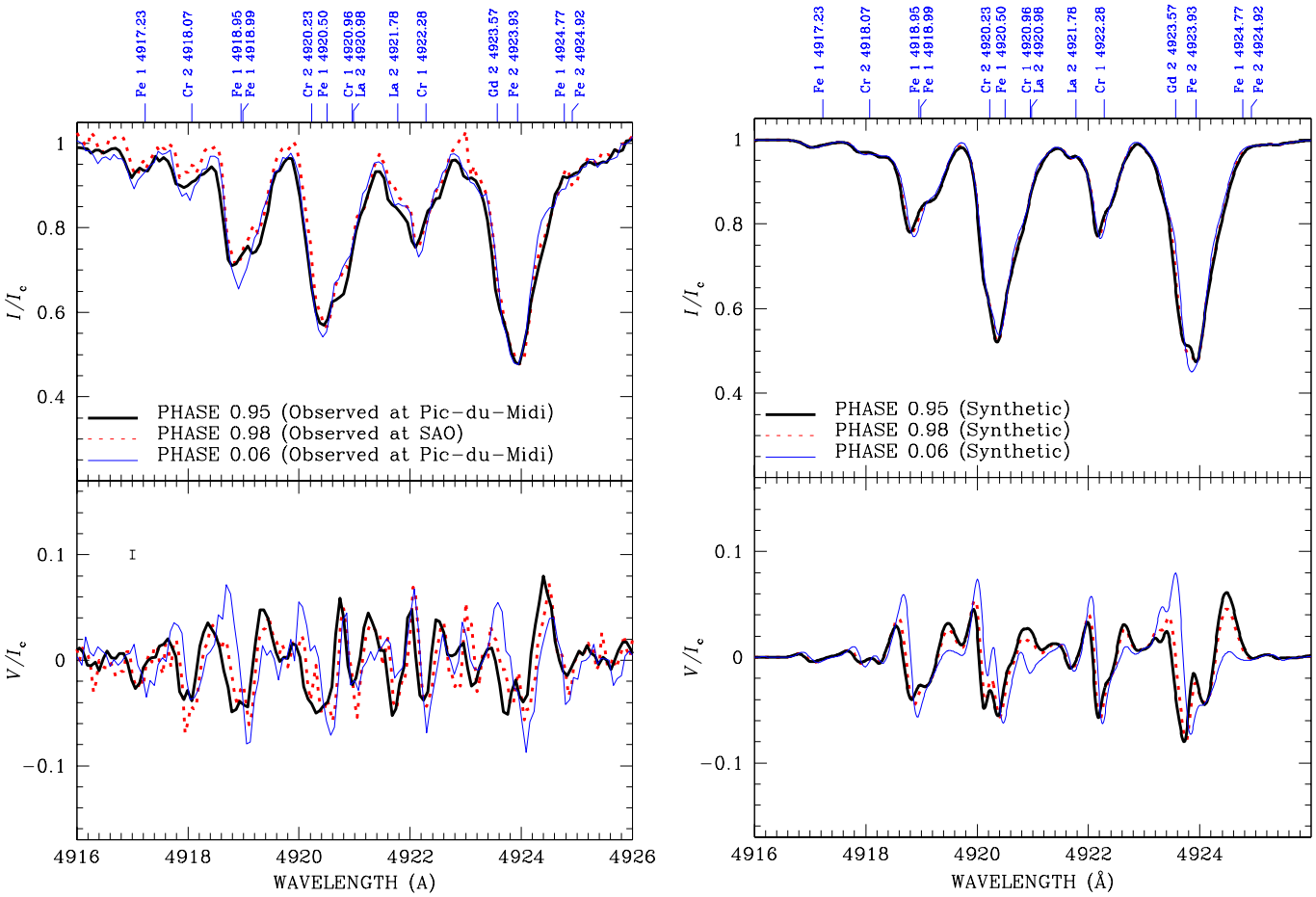

Fig. 1. Left panels: comparison of observed Stokes I and V obtained at Pic-du-Midi and at SAO in the spectral region around 4921 Å for 53 Cam. Thick solid lines: Pic-du-Midi spectra at phase 0.95; dotted lines: SAO spectra at phase 0.98; thin solid lines: Pic-du-Midi spectra at phase 0.06. In the lower panel it is also indicated the typical error bar for Stokes V as obtained at Pic-du-Midi. Right panels: predictions of the magnetic model of Eq. (1) for the same rotational phases (see Sect. 6.1.5) show that the observed differences in Stokes V can be explained in terms of the star's magnetic variability (symbols as for left panels)

importance of these different contributions, we used the magnetic field model for 53 Cam described by Eq. (1) (discussed later in this paper in Sect. 6.1.5) as a basis for computing synthetic Stokes I and V spectra corresponding to the three observed rotation phases (the details of this synthesis procedure will be explained later). These synthetic Stokes I and V spectra are shown in the right panels of Fig. 1. Despite the lack of detailed agreement between the synthetic and observed spectra (which is one of the primary themes of this paper and will be discussed later) one can clearly see that the degree of observed differences among the Stokes I and V spectra is at the same level of what can be ascribed to the variation of the visible magnetic configuration. In particular it should be noted that the differences between Stokes V taken at phase 0.95 and 0.98 are generally consistent with the typical error bar (shown in the left bottom panel). This suggests that any systematic instrumental or processing differences (except the difference in spectral resolution, which is clearly detected and which is accounted for in the synthetic calculation) between the Pic-du-Midi and SAO spectra are probably similar to or below the noise level.

4. Field modelling procedure and input physics

4.1. Modelling of the magnetic observables

To model the magnetic field we employ the least-squares method for the inversion of the magnetic observables presented by Landolfi et al. (1998) and Bagnulo et al. (2000), which we briefly outline in this section.

The stellar magnetic field is assumed to result from the superposition of a dipole field and a (non-axisymmetric) quadrupole field (see Bagnulo et al. 1996, for the generalisation to an arbitrary multipolar order). The orientation of the rotation axis as well as the orientation and strength of both the dipole and quadrupole are all free parameters to be determined by the least-squares technique.

The calculation of the longitudinal field, crossover, quadratic field and mean field modulus does not require spectrum synthesis, as these observables can be calculated directly from the assumed magnetic geometry and limb darkening. The BBLP signal observed in β CrB and 53 Cam (Leroy 1995a) is assumed to result from differential saturation of the σ and π components of the

Zeeman-split spectral lines (Leroy 1962; Calamai et al. 1975; Landi Degl'Innocenti et al. 1981). In the inversion procedure, the modelling of the BBLP observations is based on the Unno-Rackowsky solution to the polarized radiative transfer equation (see Landolfi & Landi Degl'Innocenti 1982). The stellar spectrum is taken to be an ensemble of identical, unblended "average" lines, characterised by the same Landé factor, the same strength η_0, and the same damping constant a. The validity of this assumption has been discussed by Bagnulo et al. (1999a). As a note of caution let us point out that the observed BBLP variations (as well as the other magnetic curves) may be affected to some extent by the presence of horizontal abundance nonuniformities (which are not accounted for in our modelling technique).

4.2. Model atmosphere properties and atomic database

Like conventional spectrum synthesis, modelling the variable, polarized spectra of CP stars requires accurate physical parameters (effective temperature $T_{\rm eff}$ and surface gravity $\log g$) to describe the stellar atmosphere, and accurate atomic data to correctly describe the line opacity. This is particularly difficult for CP stars for various reasons. First, the relative uncertainties associated with $T_{\rm eff}$ and $\log g$ are typically 2–5 times higher than for "normal" upper main sequence stars. Second, spectra of CP stars often contain lines of chemical elements or ions (e.g., rare earths) for which accurate atomic data (often including wavelengths!) are unavailable. A possible third difficulty is that the nonuniform magnetic field and abundance distributions modify the structure of the atmosphere, which makes questionable the appropriateness of conventional atmosphere models.

For both stars we employ ATLAS9 model atmospheres with no convection and metallicity globally enhanced by 1.0 dex. For β CrB, the atmospheric parameters are $T_{\rm eff} = 7800$ and $\log g = 4.25$ ("average" values from various reliable estimates given in the literature, e.g., Hauck & North 1982, 1993; Adelman 1985; Faraggiana & Gerbaldi 1993), while for 53 Cam they are $T_{\rm eff} = 8500\,{\rm K}$ and $\log g = 4.00$ (Landstreet 1988). Model continuous opacities are also obtained from ATLAS9, and are consistent with the adopted model atmospheres.

All the atomic data have been taken from the VALD database (Piskunov et al. 1995).

4.3. The polarized spectrum synthesis code

We have made use of the Ada95 code COSSAM (Stift 2000), slightly modified in order to accommodate a magnetic morphology described in terms of a multipolar expansion. For the formal solution of the polarized radiative transfer equation, both the DELO (Rees et al. 1989) and Zeeman-Feautrier (Auer et al. 1977) solvers are implemented in COSSAM. Following the arguments and evidence in favour of the latter solver presented by Stift (1998) and Wade et al. (in preparation), we performed our calculations using the Zeeman-Feautrier solver. Accuracy and performances of COSSAM have been thoroughly checked also by means of comparisons with the outputs of two other (independent) codes for polarized spectrum synthesis, i.e., ZEEMAN (Landstreet 1988) and INVERS10 (e.g., Piskunov 1999) – the results of this work will be presented by Wade et al. (in preparation).

For the spatial (disc integration) grid, COSSAM adopts the optimised algorithm described by Stift (1985) and Fensl (1995). This algorithm distributes the spatial grid points in such a way as to guarantee optimum spatial integration in the presence of rotational and/or pulsational Doppler shifts on the one hand, or of variations in magnetic field strength and direction on the other hand. In the present work, this adaptive spatial grid consists of about 500 points. The spectral (wavelength) grid is equispaced with a 0.01 Å step size. All lines contained in the VALD database (Piskunov et al. 1995) which exhibit central opacity exceeding 1% of the continuum opacity at any depth in the atmosphere were included in the spectrum synthesis.

A homogeneous distribution of all chemical elements over the stellar surface has been assumed throughout.

The microturbolence was set to $0\,{\rm km\,s^{-1}}$.

The calculated Stokes profiles (which conform to the definitions of Shurcliff 1962) have subsequently been convolved with a Gaussian instrumental profile, the FWHM of which corresponds to a spectral resolution of $R = 35\,000$ for the Pic-du-Midi spectra and of $R = 40\,000$ for the SAO spectra.

5. β Coronae Borealis

5.1. Magnetic field inferred from the magnetic observables

From the inversion of the magnetic observables Bagnulo et al. (2000) obtained two models for the magnetic configuration of β CrB. The parameter sets describing these models are given by Bagnulo et al. (2000) in their Eqs. (22) and (23), and the corresponding magnetic maps are shown in their Figs. 3 and 4.

Both of these models have been used as input to the synthesis code COSSAM in order to calculate model predictions to compare with the observed Stokes profiles.

5.2. Synthetic vs. observed Stokes profiles

We started our investigation by producing a synthetic spectrum spanning the spectral region 4500–6500 Å, (i.e. the approximate MuSiCoS spectral window) using the magnetic model of Eq. (22) (of Bagnulo et al. 2000) at phase 0.012.

Striking inconsistencies were found when we compared Stokes I to the observations. The observed wings of strong metallic spectral lines are often much broader than predicted by the model, and a wealth of weak lines present

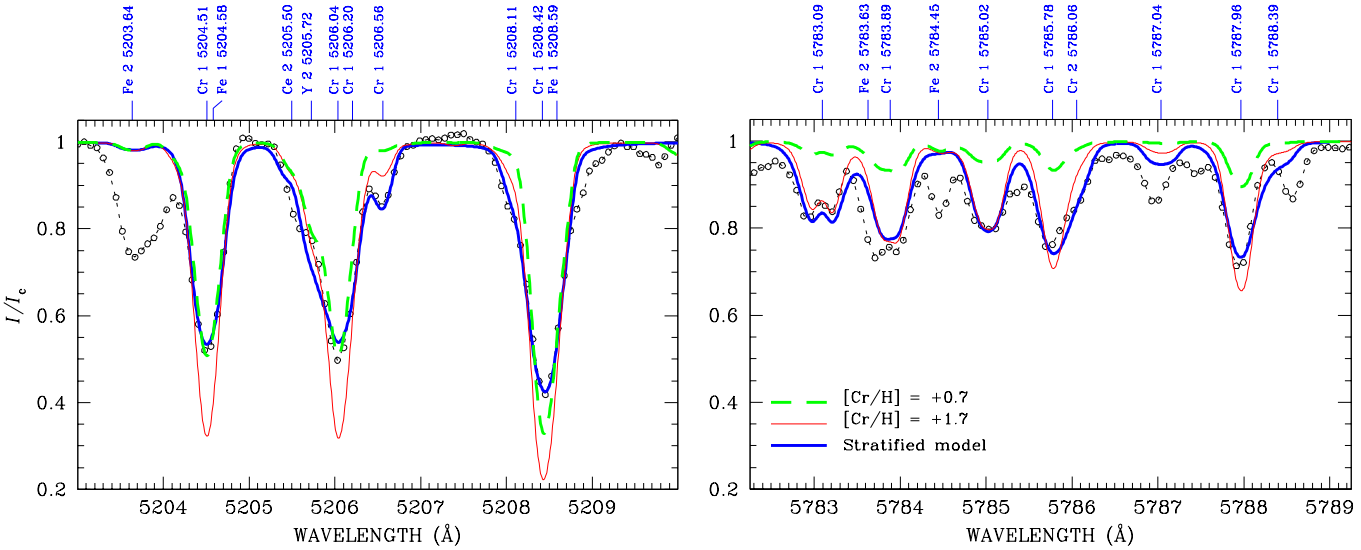

Fig. 2. β CrB: comparison of synthetic vs. observed Stokes I for two selected spectral regions including Cr I lines of different strength. Empty circles, connected by dotted lines, show the observed spectrum. Dashed lines show synthetic Stokes I calculated assuming a Cr I abundance enhanced by a factor of +0.7 dex with respect to the solar case, i.e., [Cr/H] = +0.7 (assuming for the solar abundance the values given by Grevesse & Anders 1991). Thin solid lines show Stokes I calculated setting [Cr/H] = +1.6. Thick solid lines refer to a two-zone stratified model obtained as follows: in the lower zone we set [Cr/H] = +2.7, in the upper zone we set [Cr/H] = −0.3, and the jump is at $\tau_c = 0.31$, where τ_c is the continuum optical depth at 5000 Å

in the observations are not accounted for in the synthetic spectrum. The central wavelengths of most such weak lines often correspond to those of known spectral lines (i.e., included in VALD), but the equivalent widths and depths of weak lines predicted by the model are far *smaller* than are observed. This cannot be generally explained in terms of a simple underestimate of the element abundances. When we adopted a value for the element abundance appropriate for a typical "average" line of an individual ion, we found that *depths of weaker observed lines tend to be underestimated by the model, whereas depths of stronger observed lines tend to be overestimated.* This phenomenon was clearly detected for spectral lines of the following ions: Ca I, Ti II, Fe I, Fe II, Cr I, Cr II, and Ce II. Adopting the element abundance which accounts for stronger Ca I lines led to calculated lines that are weaker than all identified, relatively weaker, Ca II lines[1].

An illustration of this phenomenon is shown in Fig. 2 for a sample of strong and weak Cr I lines. Dashed lines show Stokes I calculated assuming for the Cr abundance a value ([Cr/H] = + 0.7; we assume the solar abundances given by Grevesse & Anders 1991) which accounts for the stronger lines displayed in the left panel; this model underestimates the weaker Cr I lines (shown in the right panel of Fig. 2). Conversely, adopting a higher value for the Cr I abundance ([Cr/H] = + 1.7) permits us to explain the weaker lines, but model predictions – shown in Fig. 2 with thin solid lines, largely overestimate the depth of stronger spectral lines. This systematic trend makes it difficult to ascribe the observed disagreement to the most obvious culprits, e.g. an inappropriate choice of stellar temperature and/or surface gravity, inaccurate oscillator strengths in the atomic database, blends with unknown spectral lines, or a mistuning of the microturbulence parameter, which is set to 0 km s^{-1} and cannot be made smaller. Nor does this phenomenon appear to result from shortcomings of the magnetic model, since the variability of the Stokes profiles of weaker lines, as we will show later, is sufficiently well accounted for to rule out magnetic intensification as the main physical agent responsible for the observed discrepancies.

Following the works of Babel & Lanz (1992) and Babel (1994), we suggest that this phenomenon can be interpreted in terms of a nonuniform distribution of these ions as a function of optical depth, i.e., *chemical stratification.* Since weaker lines are formed at larger optical depths than stronger lines, the observed trend fits qualitatively a scenario in which elements are more abundant deeper in the photosphere than in the outer layers. To test this hypothesis we have performed new calculations of Fe I and Fe II, Cr I and Cr II, and of Ca I and Ca II using simple two-zone stratified models (e.g. Babel 1994). Strong and weak spectral lines of all these ions are substantially better reproduced by chemically stratified models than by unstratified models. The stratified models are typically characterised by an abundance contrast of about 3 dex between the upper and lower "zones". Synthetic Stokes I spectra, calculated for a chemically stratified Cr distribution, are also shown in Fig. 2, with thick solid lines.

[1] In fact, for virtually *all* identified ions, we could not recover a unique value of the element abundance accounting for all observed lines of the individual ion. A more accurate analysis – which is outside the scope of this paper – is necessary to establish whether there exists a trend similar to that exhibited e.g. by Cr I.

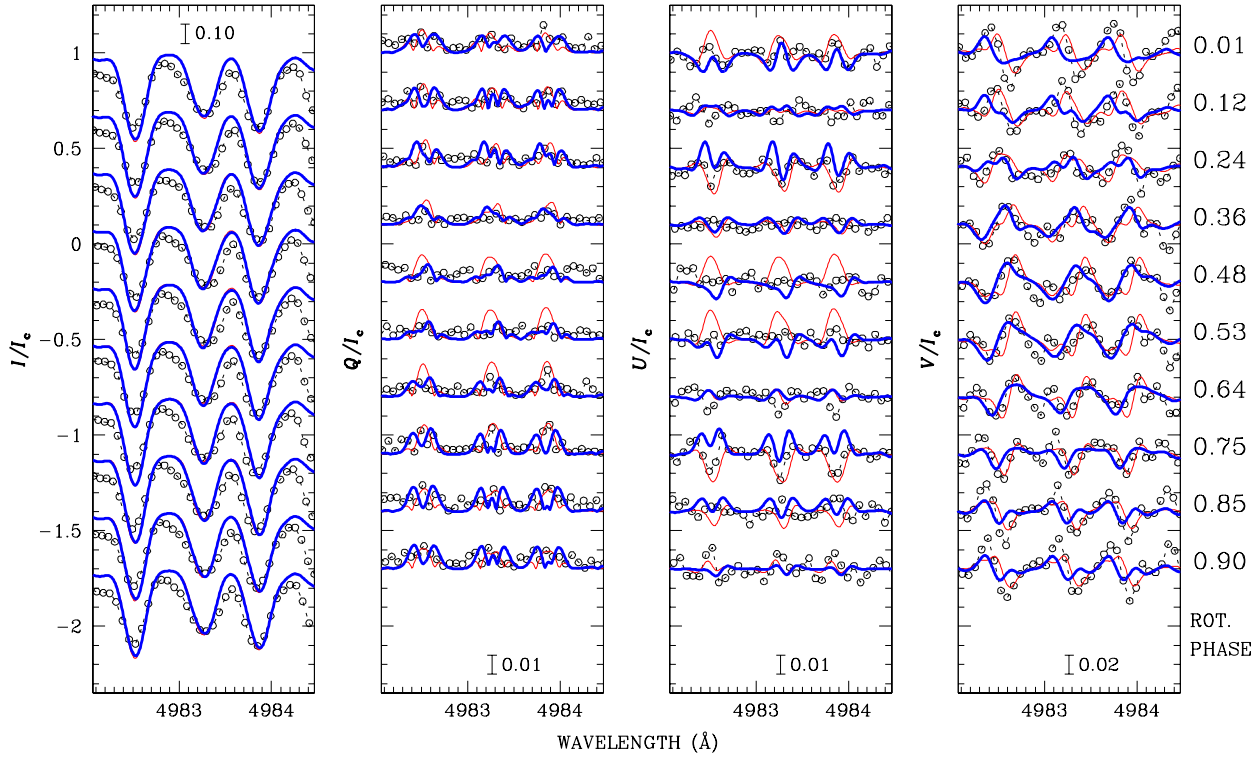

Fig. 3. β CrB: Stokes profiles for three Fe I lines around 4893 Å. Synthetic spectra are calculated setting [Fe/H] = +0.6

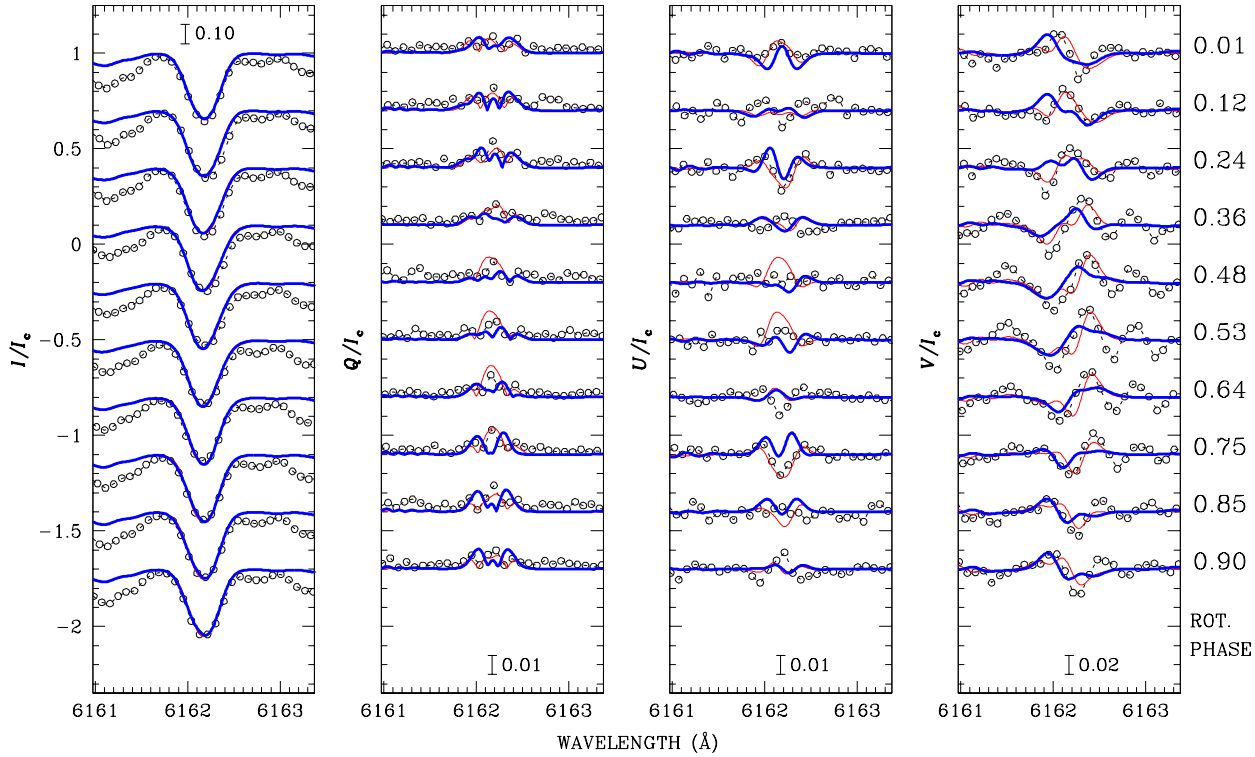

Fig. 4. β CrB: Stokes profiles for the Ca I line at 6162.173 Å. Synthetic spectra are calculated setting [Ca/H] = +0.1

Abundance stratification is expected to result naturally from microscopic chemical diffusion, and has been examined by Babel & Lanz (1992) and Babel (1994), and more recently by Savanov & Kochukhov (1998). Admittedly, it came as a surprise the dramatic impact that stratification has on the spectrum of β CrB, which suggests that abundance analyses of this star (and probably many other CP stars) performed without accounting for it will be completely misleading, and should be revisited. We are presently undertaking a more complete study

of stratification in a sample of magnetic and non-magnetic CP stars (including β CrB). Work in this direction is also currently in progress by Ryabchikova et al. (in preparation).

Stratification effects are clearly very important. However, a proper modelling requires an extensive investigation which is outside the scope of the present work. For a detailed comparison of a time series of synthetic vs. observed Stokes $IQUV$ profiles, we decided to use a value of the element abundance specifically chosen in order to best reproduce each individual line profile, regardless of the consistency with the abundance as obtained from other spectral lines of the same ion. Numerical simulations showed that this is an adequate approximation for weak lines, in which case stratification affects mainly the depth of Stokes profiles, but not their shape. By contrast, for strong lines, stratification changes also the *shape* of Stokes profiles, in particular, Stokes QUV appear like smeared out compared to the non stratified case.

For weaker lines, Stokes I profiles predicted by both magnetic models agree more or less satisfactorily with the observations of β CrB. The agreement of the remaining three Stokes parameters (which are much more sensitive to the magnetic geometry than Stokes I) is less satisfactory than for Stokes I. Figure 3 shows observed and calculated profiles of three Fe I lines around 4983 Å. Empty circles represent the observations, and the model predictions are represented by thin solid lines (model of Eq. (22) of Bagnulo et al. 2000) and thick solid lines (model of Eq. (23)). The four panels, from left to right, show Stokes I, Q, U, and V, normalised to the continuum I_c. The scale adopted for Stokes V is five times larger than for Stokes I, while that adopted for Stokes Q and U is ten times larger than for Stokes I. From top to bottom, the profiles refer to increasing rotation phases, as indicated on the right side of the rightmost panel (for display purposes we selected only 10 phases, although all 17 observed phases have been compared with the model predictions). Phase 0.0 corresponds to J.D. = 2450011.06, with an assumed stellar period of 18.4866 d (Bagnulo et al. 2000). Figure 4 shows a similar example for the Ca I line at 6162.217 Å. Zeeman splitting is clearly detected in the Fe II line at 6149.258 Å (the line employed by Mathys et al. 1997) to infer the mean magnetic field modulus of 42 CP stars), and also reasonably well accounted for, as shown in Fig. 5[2].

[2] Note the absence of linear polarization signatures in this line. This comes from the fact that the line is fully split (locally, at any point of the stellar surface) into two components, + and −, each of which is the superposition of a π and a σ component. Radiative transfer in the + component is independent of radiative transfer in the − component (e.g., Mathys 1989). In each component, the form of the polarized radiative transfer equation is such that Stokes I and V are coupled to each other, and Stokes Q and U are coupled to each other, but the two pairs (I, V) and (Q, U) are independent. With the boundary condition that at the bottom of the atmosphere, the radiation is unpolarized, no linear polarization is generated.

Based in Figs. 3, 4 and 5, we conclude that the magnetic field models for β CrB obtained from the magnetic observables reproduce only approximately the observed Stokes $IQUV$ profiles of weak lines.

For strong lines, even Stokes I could not always be satisfactorily reproduced. Several of the singly ionized lines of Fe, viz. Fe II 4923.927 Å, Fe II 5018.440 Å, and Fe II 5169.033 Å, (which incidentally belong to the same multiplet, #42) yield particularly unsatisfactory fits. Figure 6 shows the example of Fe II 4923.927 Å. For both models, synthetic Stokes I profiles appear blue-shifted with respect to the observations. However, a similar shift is not observed in other strong spectral lines (see Fig. 2). The observed shift is likely an artifact due to a blend with a spectral line in the red wing (possibly Ce I), or to an overestimate of the abundance of a Gd II line which is included the spectral synthesis in order to explain the blue wing the line, in combination with important effects of chemical stratification which are not taken into account. A detailed model of this line will be presented by Wade et al. (in preparation).

Similar problems were encountered, e.g., with Na I 5889.951 Å, Mg I 5172.684 Å, Ba II 6151.173 Å. We could not reproduce the shape of Stokes I in these lines, neither in the core nor in the wings. A good fit to the line wings results in substantially deeper profiles than are observed, and a good fit to the core results in line wings which are much less broad than those observed. Again, this can be understood in terms of chemical stratification, as wings of strong lines are formed deeper in the photosphere than is the line core. A stratified model could fit the observations essentially by allowing the weak lines formed at depth to be reproduced with the high abundance assumed, while the *cores* of strong lines, normally dark because they are formed far out in the atmosphere where the LTE source function is weak, are weakened because there is little opacity in the outer layer to drive the line centres down – this is why the abundance contrast between the two layers has to be as large as some dex.

One might infer that our failure to account for chemical stratification would impact strongly our ability to judge the reliability of the magnetic models, since the most prominent Stokes Q and U signatures are observed in strong lines, and those lines are the most strongly influenced by stratification. In fact, we found that the comparison of synthetic vs. observed Stokes QUV profiles for both strong and weak lines leads to qualitatively similar conclusions: the model of Eq. (22) (thin solid lines) is uniformly at odds with the observed linear polarization at rotation phases 0.48, 0.53, 0.64, and 0.75, while the model of Eq. (23) (thick solid lines) presents strong deviations from the linear polarization features observed at rotation phases 0.36 and 0.64, and Stokes V appear systematically slightly blue-shifted with respect to the observations. Less glaring inconsistencies with the observations are ubiquitous throughout the rotational cycle for both models, and it does not seem possible to ascribe these discrepancies to a horizontal modulation of the element abundances (see

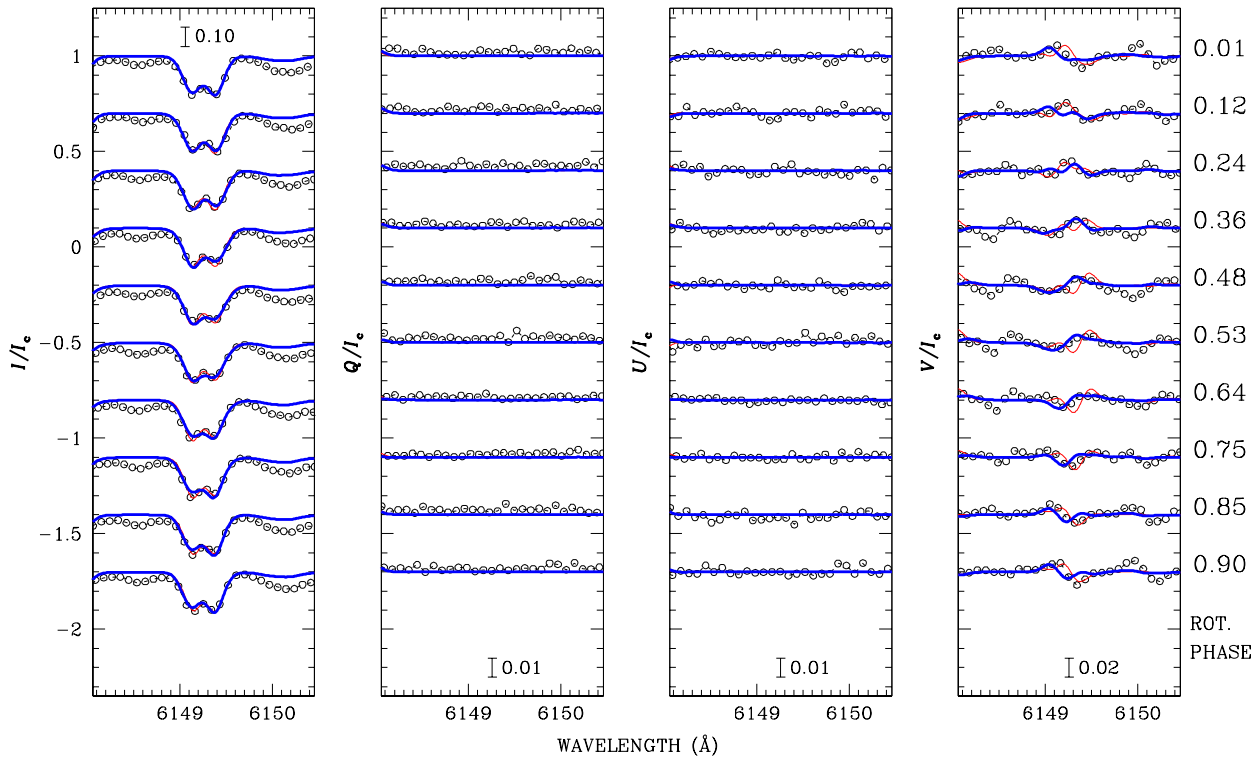

Fig. 5. β CrB: Stokes profiles for the Fe II line at 6149.258 Å. Synthetic spectra are calculated setting for [Fe/H] = +0.6

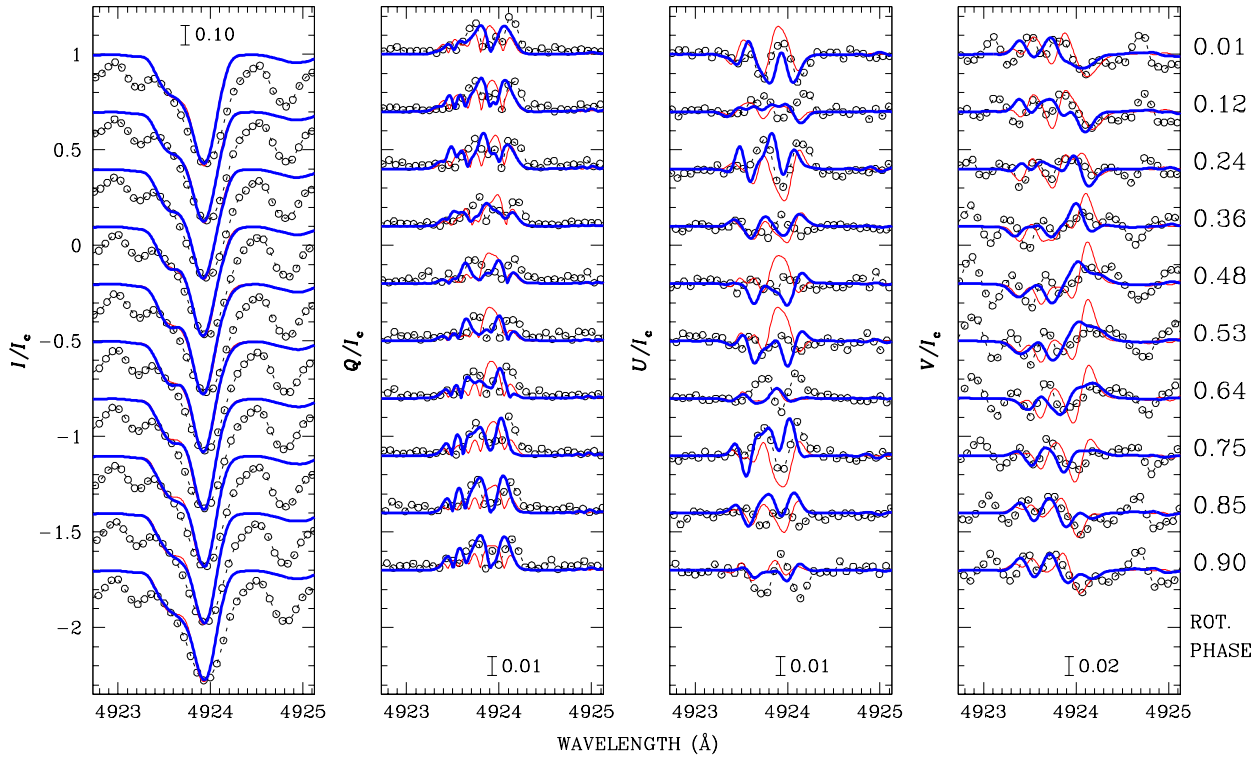

Fig. 6. β CrB: Stokes profiles for the Fe II line at 4923.927 Å. Synthetic spectra are calculated setting for [Fe/H] = −0.6

Sect. 7). On the whole, the discrepancies between predictions and observations are of similar magnitude for both models, so that we are not even able to indicate which one of the models – if either – is the more realistic one.

6. 53 Camelopardalis

Landstreet (1988) proposed an axisymmetric magnetic field plus abundance distribution model for 53 Cam, which was found by Wade et al. (2000a) to be inadequate to

explain the observed Stokes $IQUV$ profiles. In an attempt to recover a more realistic magnetic topology for 53 Cam, we present a new modelling based the second-order, non axisymmetric multipolar expansion described by Bagnulo et al. (2000).

6.1. Modelling the magnetic observables

6.1.1. Determinations of longitudinal field

Two procedures, both based on observations of circular polarization, have traditionally been used in the determination of the mean longitudinal magnetic field. These are referred to as the "photographic technique" and the "photopolarimetric technique", and are described, e.g., by Mathys (1989) and by Landstreet (1992). For 53 Cam, measurements of both kinds are available in the literature.

Eleven observations of the longitudinal field were made by Babcock (1958) by means of the photographic technique. An additional 33 observations were later obtained by the same author, but are only available in the form of a plot (see, e.g., Babcock 1960b). With a similar technique, eight longitudinal field determinations were performed by Preston & Stępień (1968), and another four by Hildebrandt et al. (1997). Wade et al. (2000c) have added ten more observations. Nine $\langle \mathcal{B}_z \rangle$ determinations have been presented in Sect. 3.4. Using the photopolarimetric method, Borra & Landstreet (1977) obtained 18 observations and Hill et al. (1998) contributed 17 additional measurements. All these observations are shown in the top left panel of Fig. 7.

It is well known that observations of the longitudinal field obtained using the photographic technique with a photographic plate as the actual detector can be subject to important systematic effects (Borra 1974). Systematic deviations may indeed be present in the observations reported by Babcock, which around phase 0.40–0.60 are inconsistent with the observations obtained by the other authors (see Fig. 7). We have therefore excluded Babcock's measurements from our analysis. Replacing the photographic plate with a CCD overcomes this problem, and dramatically increases the precision of the measurements. Still, magnetic fields deduced from spectropolarimetric observations of metallic lines may be affected by a non-uniform distributions of the chemical elements over the stellar surface, and can be furthermore quite sensitive to blending.

Photopolarimetry in the Balmer lines overcomes some of these problems: H is the dominant constituent of the stellar atmosphere, and should therefore be distributed approximately homogeneously over the stellar surface. However, Musielok & Madej (1988) found that the Strömgren β index (which reflects the equivalent with of Hβ) is periodically variable for most magnetic CP stars, and Leone & Manfrè (1997) have suggested that metal rich and/or helium enriched or depleted regions can modify Balmer lines, resulting in uncertainties of longitudinal fields obtained via the photopolarimetric technique of up to 10% (in fact, such an uncertainty is comparable in magnitude to the uncertainties associated with the inference of the longitudinal field from the measured photopolarization – see, e.g., Borra & Landstreet 1977).

Recently, Mathys et al. (2000) and Brillant et al. (1999) have argued that the theoretical approaches to the interpretation of Balmer line observations in terms of a longitudinal field are incomplete, since they actually rely on a weak-field solution of a form of the equation of transfer of polarized radiation which is valid for atoms undergoing pure Zeeman effect. In fact, one should also include the Stark effect due to the perturbation of the hydrogen atoms by charged particles of the stellar atmosphere, and the Lorentz effect (resulting in an induced electric field) due to the thermal motion of the radiating atom in the magnetic field.

In addition, it should be recalled that 53 Cam is a spectroscopic and astrometric binary (SB1; Scholz & Lehmann 1988; Martin & Mignard 1998). Inspection of our spectra results in no evidence for a significant contribution by the secondary to the observed line profiles. It is however possible that there is some contribution (either a modification of the profile shape, or a dilution of the line and the associated polarization due to the companion's unpolarized flux) by the companion to the observed Hβ profile. Unfortunately, we are not able to estimate quantitatively its effect on the longitudinal field values, but it is probably relatively small given the large mass ratio and hence the presumably large flux ratio (e.g., Martin & Mignard 1998).

For many stars, major discrepancies have been noted between longitudinal field values determined with the "photographic" and "photopolarimetric" techniques (Mathys 1991). In the particular case of 53 Cam, there is evidence for only a marginal inconsistency – in the vicinity of the longitudinal field maximum. Whether this discrepancy is due to a shortcoming of the photopolarimetric technique or rather of the photographic technique (or perhaps of both!) is impossible to decide.

6.1.2. Determinations of the mean field modulus

The determination of the mean field modulus $\langle \mathcal{B} \rangle$ is based upon observations of fully or partially resolved Zeeman patterns in Stokes I spectra. The first measurement of the mean field modulus of 53 Cam was published by Preston (1969), followed by Huchra (1972) with 20 observations and Mathys et al. (1997) with 16 more $\langle \mathcal{B} \rangle$ determinations (one of these, obtained on JD = 2449253.001, is not included in our analysis because it appears to be inconsistent with the overall smooth nature of the magnetic curve). Note that the $\langle \mathcal{B} \rangle$ values given by Mathys et al. (1997) are derived solely from the splitting of the Fe I line at 6149 Å. This is a particular difficult task in 53 Cam, owing to a strong blend in the blue wing of the line (Mathys et al. 1997). Furthermore, it should be noted that in presence of a such a strong field as observed in 53 Cam, the formation

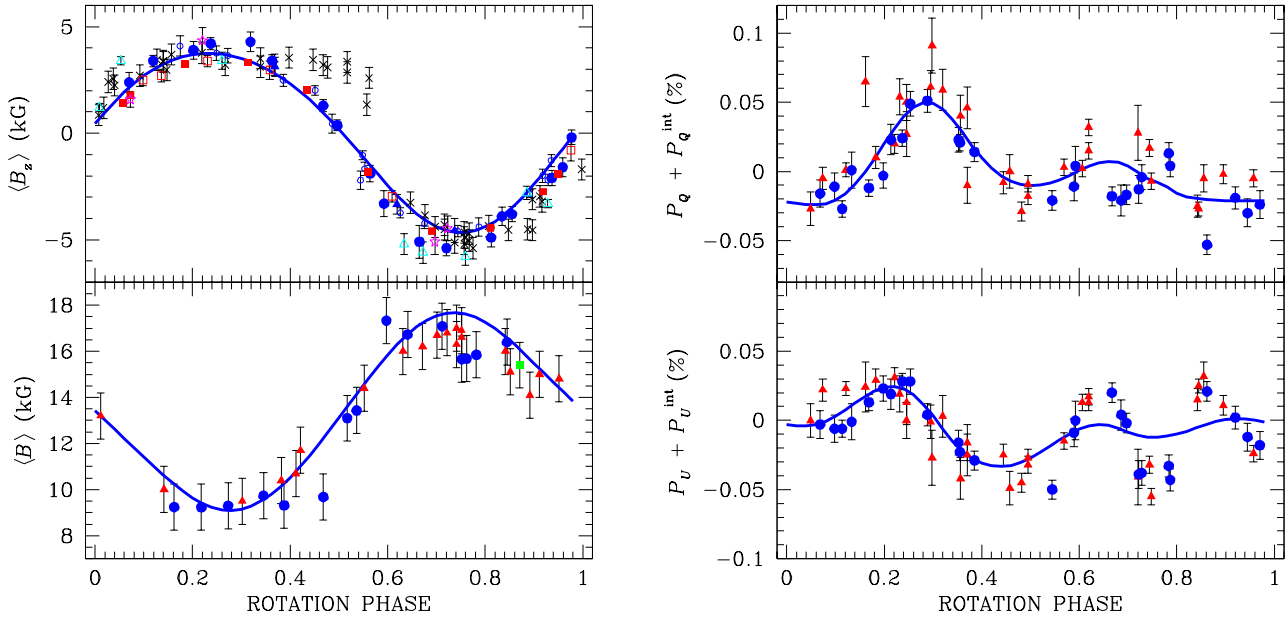

Fig. 7. Modelling the magnetic observables of 53 Cam. In the panel corresponding to the longitudinal field $\langle \mathcal{B}_z \rangle$, symbols are as follows. Crosses: Babcock (1958, 1960b); empty triangles: Preston & Stępień (1968); filled circles: Borra & Landstreet (1977); empty stars: Hildebrandt et al. (1997); empty circles: Hill et al. (1998); filled squares: Wade et al. (2000c); open squares: this work (from SAO spectra) filled triangles: this work (from Catania spectra). For the mean field modulus $\langle \mathcal{B} \rangle$ (left bottom panel), the filled square represents the measurement by Preston (1969), filled triangles the observations by Huchra (1972), filled circles those by Mathys et al. (1997). For the BBLP measurements (right panels), filled triangles are the measurements by Kemp & Wolstencroft (1974), filled circles the measurements by Leroy (1995a). Solid lines display the calculated magnetic curves for the adopted magnetic model, of Eq. (1)

of the Fe II 6149 Å line occurs in Paschen-Back regime, which is not taken into account in the technique for the determination of the mean field modulus. (The impact of partial Paschen-Back effect on the spectra of CP stars is currently under study by Landolfi et al., in preparation.) Nevertheless, all data sets are fully consistent among themselves. We estimate that the uncertainty in the determinations of the mean field modulus of 53 Cam is 1.0 kG. All measurements of mean field modulus as shown in the left bottom panel of Fig. 7.

6.1.3. Observations of broadband linear polarization

53 Cam was the first star to be monitored in BBLP throughout an entire rotation cycle, by Kemp & Wolstencroft (1974), who obtained 32 observations through an extended Johnson B filter. Leroy (1995a) published 27 new measurements obtained through a standard Johnson B filter. All data are shown in the right panels of Fig. 7. We note a certain lack of consistency among the two sets of observations which – as already pointed out by Leroy (1995a) – might be due to the slightly different filters employed. Furthermore, BBLP measurements appear to have a larger scatter than the nominal error bars. In particular the errors bars associated to the measurements by Kemp & Wolstencroft (1974) may be somewhat underestimated (see Leroy 1995 for a similar comment). Finally, a comparison of the BBLP observations of 53 Cam with quantitative theoretical predictions (see Bagnulo et al. 1995) shows that the observed BBLP signal is much smaller than expected. In principle, this could be explained in part by dilution of the polarized radiation by the (probably unpolarized) flux of the secondary. (For a general discussion of the impact of a companion on modelling the BBLP measurements we refer the reader to Bagnulo et al. 2000.) However, as we shall see later, binarity is in fact unlikely to be the sole depolarising agent.

6.1.4. Other observational data

For the rotation period we adopted the value of 8.02681 ± 0.00004 obtained by Hill et al. (1998) who fitted a first-order Fourier expansion to a homogeneous set of photopolarimetric $\langle \mathcal{B}_z \rangle$ measurements. Landstreet (1988) obtained the projected rotational velocity for 53 Cam, $v_e \sin i = 13.0 \pm 1.5\,\mathrm{km\,s^{-1}}$; he also provided an estimate of the limb-darkening coefficient ($u = 0.575$). For the stellar radius we assumed $R_* = 2.56 \pm 0.30$ (Hubrig et al. 2000), a value consistent with Landstreet's (1988) results.

6.1.5. Field modelling results

Along the lines suggested by Bagnulo et al. (2000), we decided to follow a two-step procedure in modelling the magnetic field of 53 Cam. In a first analysis we neglected the observations of BBLP, i.e., we started our analysis by looking for models giving a simultaneous best fit to the observations of the longitudinal field $\langle \mathcal{B}_z \rangle$ and of the field modulus $\langle \mathcal{B} \rangle$. In order to take into account possible systematic differences in the $\langle \mathcal{B}_z \rangle$ values based on one or the

other of the two techniques discussed above, we decided to distinguish three different cases. In the first case, we considered only the photopolarimetric $\langle \mathcal{B}_z \rangle$ determinations of Borra & Landstreet (1977) and of Hill et al. (1998). In the second case, we considered only the "photographic" $\langle \mathcal{B}_z \rangle$ values of Preston & Stępień (1969), Hildebrandt et al. (1997), Wade et al. (2000c), and those reported in Table 1 of this work. Finally, in the third case, we considered all of the available $\langle \mathcal{B}_z \rangle$ observations (but those by Babcock, see Sect. 6.1.1). In the second step, we also included the BBLP observations in determining the model.

We found that the model characterised by the lowest value of the reduced χ^2 was that obtained by neglecting the BBLP observations and by considering only the photopolarimetric $\langle \mathcal{B}_z \rangle$ measurements (along with the $\langle \mathcal{B} \rangle$ measurements; $\chi^2/\nu = 1.0$). The best model obtained by including all $\langle \mathcal{B}_z \rangle$ measurements was characterised by a much larger value of the best-fit reduced χ^2 ($\simeq 2.8$). Including the BBLP measurements led to even higher χ^2 values. This can only partially be explained in terms of underestimate of their error bars (see Sect. 6.1.3): the discrepancies between model fits and observations rather suggest that our framework is still too simple to reproduce the observed magnetic curves.

Among the various solutions, we report here that which provides the best fit to all of the magnetic curves (including the BBLP), neglecting the photographic determinations of $\langle \mathcal{B}_z \rangle$, and adopting for the line strength and damping constant the values $\eta_0 = 10$ and $a = 0.0$, respectively. As "average" Landé factor we considered $g_{\rm eff} = 1.0$, and the Zeeman splitting was normalised to the Doppler width by setting $b = 3330\,\mathrm{G}$ (see Eq. (12) of Bagnulo et al. 2000). The other model parameters are:

$$
\begin{array}{rcrcl}
i & = & 117^\circ & \pm & 2^\circ \\
\Theta & = & 139^\circ & \pm & 2^\circ \\
\beta & = & 89^\circ & \pm & 1^\circ \\
f_0 & = & 80^\circ & \pm & 1^\circ \\
\beta_1 & = & 40^\circ & \pm & 2^\circ \\
\beta_2 & = & 61^\circ & \pm & 2^\circ \\
\gamma_1 & = & 96^\circ & \pm & 3^\circ \\
\gamma_2 & = & 52^\circ & \pm & 2^\circ \\
B_{\rm d} & = & 15\,440 & \pm & 350\,\mathrm{G} \\
B_{\rm q} & = & 19\,920 & \pm & 460\,\mathrm{G} \\
v_{\rm e} & = & 14.7 & \pm & 0.6\,\mathrm{km\,s^{-1}} \\
P_Q^{\rm int} & = & -5.7\ 10^{-4} & \pm & 0.4\ 10^{-4} \\
P_U^{\rm int} & = & -1.7\ 10^{-4} & \pm & 0.5\ 10^{-4}\ ;
\end{array}
\qquad (1)
$$

for the precise definitions of the various parameters, see Bagnulo et al. (2000) and Landolfi et al. (1998); here we just recall that i and Θ represents the tilt and the azimuth angle of the rotation axis, respectively; β is the angle between the dipole axis and the rotation axis, f_0 the zero point phase; (β_1, γ_1) and (β_2, γ_2) specify the orientation of the quadrupole, $B_{\rm d}$ and $B_{\rm q}$ are the dipole and quadrupole strength, respectively; $v_{\rm e}$ is the equatorial velocity, and $P_Q^{\rm int}$ and $P_U^{\rm int}$ represent the contribution of the interstellar BBLP. The associated value of the reduced χ^2 for this adopted model is 3.6, and the corresponding model predictions are shown in Fig. 7 with solid lines. An inconsistency is apparent in the recovered model line blocking factor ($\xi = 0.02$), which is four times lower than that estimated from our SAO spectra in the B band. If we fix the line blocking factor at the observed value, the model produces a much greater intensity of BBLP than is observed[3]. Binarity plays some (probably minor) rôle in the dilution of the observed linear polarization signal, and blending will also tend to reduce the BBLP with respect to that predicted under the "single-line" approximation (Leroy 1990). Nevertheless, there is no doubt that the disagreement between the observed and predicted line blocking factors (or alternatively between observed and predicted BBLP intensities) represents a shortcoming of the magnetic model. This is reflected by the high value of the reduced χ^2. Note that our difficulty in reproducing the magnetic curves also results in unrealistically small values for the model parameter uncertainties (see Bagnulo et al. 2000, for similar comments regarding β CrB). It should be furthermore noted that not only does the model of Eq. (1) fail to reproduce satisfactorily the magnetic curves, but neither can it be deemed *unique*. We found that the modelling results were dependent both on the set of $\langle \mathcal{B}_z \rangle$ measurements adopted, and on the choice of the (fixed) values of η_0, a and b. From this point of view, adopting the particular set of parameters of Eq. (1) is a somewhat arbitrary choice. On the other hand, a representative example of the modelling results is necessary in order to perform a comparison with the Stokes profiles – and, as we shall see shortly, none of the recovered models predicts Stokes profiles which agree well with the observations.

6.2. 53 Cam: synthetic vs. observed Stokes profiles

Using a procedure similar to that employed for β CrB, we first produced a synthetic spectrum in the range 4500–6500 Å, and we performed a preliminary comparison with the observed Stokes I spectra of 53 Cam at phase 0.08. We discovered a phenomenon similar to that observed for β CrB, i.e., we found that it was impossible to account for spectral lines of identical ions by adopting a unique value for the element abundance.

These systematic discrepancies between abundances derived from weak and strong lines are analogous to those of β CrB. As we have discussed, this phenomenon is consistent with chemical stratification (for a detailed study of chemical stratification in 53 Cam see Babel & Lanz 1992). However, this signature of stratification in the spectrum of 53 Cam is less dramatic than for β CrB, and so a vertically uniform chemical abundance model reproduces the Stokes I spectrum of 53 Cam much more coherently than for β CrB.

[3] Equation (4) of Landolfi et al. (1993) shows that the amplitude of the BBLP is proportional to the line-blocking factor ξ.

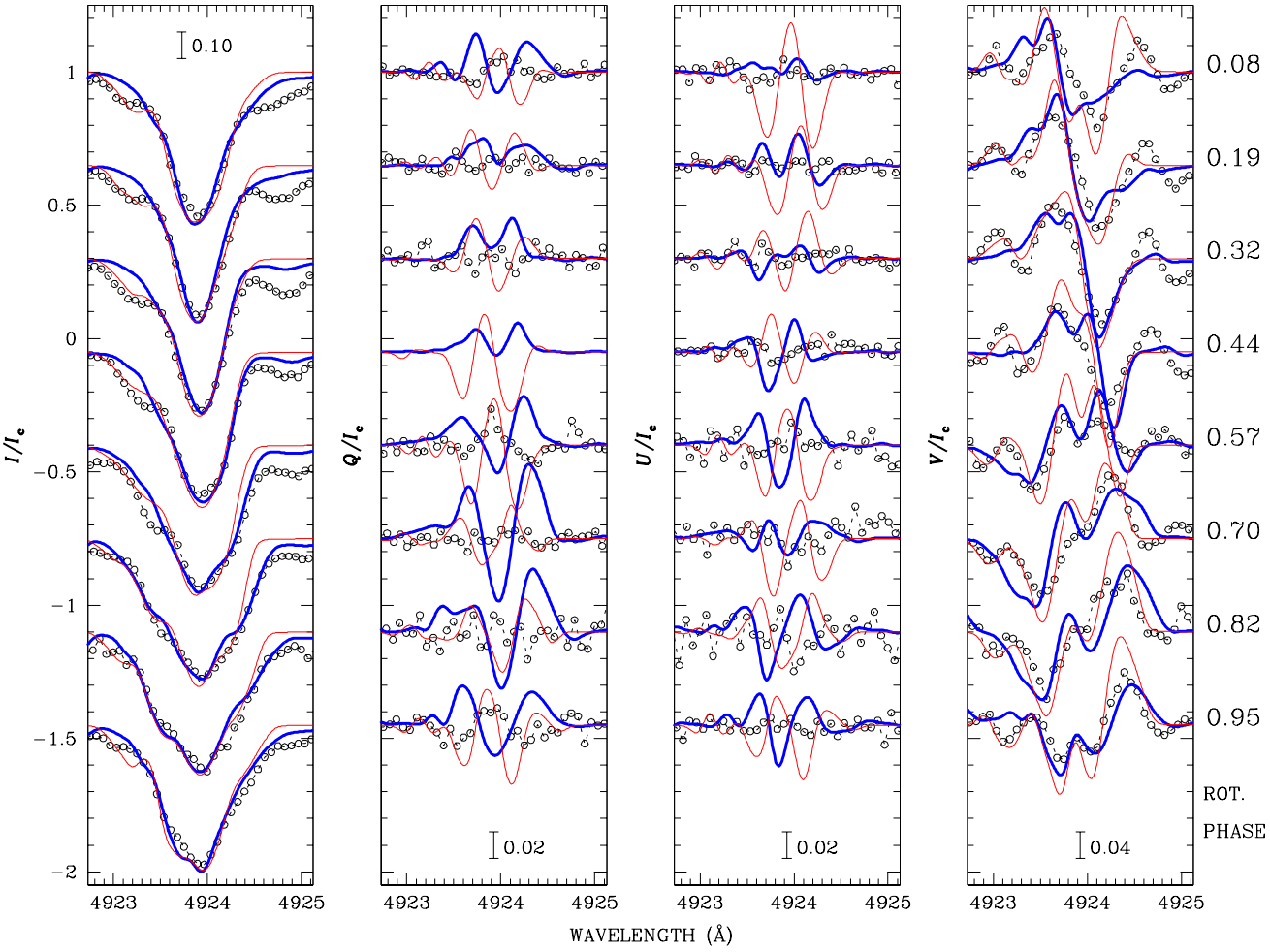

Fig. 8. 53 Cam: Stokes profiles of the Fe II line at 4923.927 Å. Synthetic spectra are calculated setting [Fe/H] = +0.1; thick solid lines refer to the model of Eq. (1), thin solid lines show the predictions of the axisymmetric model presented by Landstreet (1988)

On the other hand, the comparison of the remaining three Stokes profiles yielded much poorer agreement, notwithstanding the better agreement for Stokes I. This is illustrated in Fig. 8, which shows Stokes $IQUV$ profiles of Fe I 4923.927 Å at eight selected rotation phases. Empty circles represent the observations, and the thick solid lines show the predictions of the model described by Eq. (1). Stokes V is expanded by a factor of 2.5 with respect to Stokes I, and Stokes Q and U by a factor of 5. Discrepancies are particularly striking in Stokes Q and U. We have repeated a comparison of predicted vs. observed Stokes profiles for many other magnetic configurations, corresponding to the various relative minima of the χ^2 hypersurface, finding results qualitatively similar to those shown in Fig. 8. All models tend to *overestimate* the linear polarization, consistent with our findings from modelling the observed BBLP. By contrast, Stokes I seems reasonably well reproduced without invoking any *horizontal* abundance variation of Fe, the abundance of which was set nearly equal to the solar abundance. The blue wing of Fe II 4923.927 Å is affected by blend with a Cr I line, which we have "empirically" reproduced by assuming for Cr an abundance increased by +2.6 dex with respect to the solar abundance. Such a value is clearly inconsistent with the observations of other Cr lines, and may reflect stratification. The red wing is partially affected by blending with Fe I and Fe II lines which are not well reproduced assuming a solar Fe abundance.

The use of a non-axisymmetric model did not lead to a significant improvement of the results presented by Wade et al. (2000a), who compared the observed Stokes profiles with the predictions of the axisymmetric model proposed by Landstreet (1988) (shown again in Fig. 8 with thin solid lines). Note the similar level of (good) agreement between the Stokes I profiles and the two models (one axisymmetric, one non-axisymmetric). This underscores that Stokes I cannot be used alone for diagnostic of magnetic field structures, and highlights the value of the full series of Stokes $IQUV$ profiles in this respect.

Lacking a unique, satisfactory magnetic model, we can only draw very tentative conclusions about the magnetic configuration of 53 Cam. According to the adopted model, there exists a large patch of strong inward field, with field strength ranging from 15 kG in the outer region of the

patch to 25 kG at its centre, visible to the observer between rotation phases 0.56−0.95. Such a feature is common to *all* the various magnetic models recovered under the different approaches discussed in Sect. 6.1.5, and as such, it might in fact actually exist! This morphological feature is similar to the one represented by the negative pole of the axisymmetric model by Landstreet (1988). However, we cannot confirm that the remaining stellar surface is characterised by a single positive magnetic pole, as the magnetic morphology visible to the observer between phase 0.08−0.44 differs amongst the various models. Possibly, the magnetic structure visible to the observer at these rotation phases is organised on a smaller scale than for the remaining phases.

7. Comments on the element abundance distributions

It seems well established that the surfaces of many CP stars exhibit inhomogeneous distributions of some chemical elements.

For β CrB such inhomogeneities, if present, would primarily appear as rotating features permanently within sight on the stellar disk, as the star's rotation axis is nearly parallel to the line of sight. Indeed, there is little (if any) variability in the spectral lines of β CrB that can be attributed to abundance nonuniformities (a possible very mild variation of Fe lines may be an exception). This makes it nearly impossible to detect such inhomogeneities in Stokes I, and one might suspect that the discrepancies observed in the remaining Stokes parameters are due to the presence of abundance patches, which would give a different weight to the polarization signal originated from different regions of the stellar disk. However, it should be noted that if strong horizontal abundance variations existed in the visible part of the stellar disk, this would likely result in polarized features which change from element to element, unless we assume all elements are distributed in the same fashion. Systematic differences amongst the Stokes profiles from element to element are not observed, for instance, for Fe I and Ca I (compare Figs. 3 and 4), nor for Stokes profiles of many other ions. Accordingly, we conclude that discrepancies between model predictions and observations of Stokes profiles are mainly due to a mere inadequacy of the magnetic models.

53 Cam represents a more interesting target, as that star is observed from a much more favourable view. The problem of deriving an abundance map for 53 Cam was explored in detail by Landstreet (1988), whose results have been used in a number of studies of the general chemical transport processes leading to such nonuniformities (e.g. Babel 1992).

According to our study, a horizontal nonuniformity of the Fe abundance is not excluded, but is *not* required in order to explain strength variability of Stokes I. The disagreement between predicted and observed Stokes I is relatively mild; given the poor agreement obtained for Stokes QUV, it makes sense to interpret it mainly in terms of limitations of the model magnetic field configuration. By contrast, spectral lines of Ti II and Ca I exhibit spectacular changes in Stokes I, a phenomenon which clearly cannot be explained by magnetic intensification alone. Landstreet (1988) demonstrated that a correlation exists between the distribution of Ti II and Ca I and the occurrence of the extrema of the longitudinal field of 53 Cam. Such a phenomenon was interpreted in terms of an overabundance (underabundance) of Ti II (Ca I) in the vicinity of the negative magnetic pole of his axisymmetric model, and an underabundance (overabundance) of the same elements near the positive magnetic pole[4]. Babel & Michaud (1992) were unable to explain these results in the framework of their "simple diffusion model", which could not explain why, for instance, calcium should be concentrated more around the (strong) negative pole, and concentrated less around the (weak) positive pole in Landstreet's axisymmetric model. Babel (1992) invoked a magnetically confined stellar wind in an attempt to explain this result. In fact, the results of this work show that caution is needed for deriving a proper correlation between abundances and magnetic patches. This concept is illustrated in Fig. 9.

The left panels of Fig. 9 show the observed Stokes I variation of Ti II 4805.085 Å and Ca I 6162.173 Å, together with the profiles predicted by the model of Eq. (1), assuming a uniform horizontal (and vertical) element distribution. The right panels of Fig. 9 show the model magnetic configuration as seen from the observer at the rotation phases corresponding to the observations. The magnetic field strength is visualised by means of different colours, with contour lines about 3 kG apart. The direction of the magnetic field is represented by unit vectors, drawn in black or gray according to their outward or inward orientation, respectively. (Note that, for display purposes, the magnetic map is visualised for a zero value of the azimuth Θ of the rotation axis.) This comparison does not exclude that Ca I (Ti II) is less (more) concentrated around the large field patch with an inwardly directed, strong magnetic field. Of note is the apparent Zeemam splitting of the observed Ti II line at phase 0.82; this is not predicted by our model (which assumes titanium be homogeneously distributed over the stellar surface). Titanium is certainly probing a region characterised by a high magnetic field strength. On the other hand, the overabundance (underabundance) of Ca I (Ti II) is *not* associated with any polar cap (a patch of positive outward field is visible at rotation phases nearer to the positive crossover than to the maximum of longitudinal field). We could tentatively speculate that they are associated with a region where the magnetic field is less structured on a large scale. It should

[4] It may be that the exclusion of anomalous dispersion in Landstreet's (1988) calculations (see, e.g., Wade et al., in preparation, for more detail) resulted in the impression that a mild Fe (and possibly Cr) abundance nonuniformity existed on the surface of 53 Cam. The exclusion of these effects may also impact the accuracy of Landstreet's Ti and Ca abundances, and abundance nonuniformities.

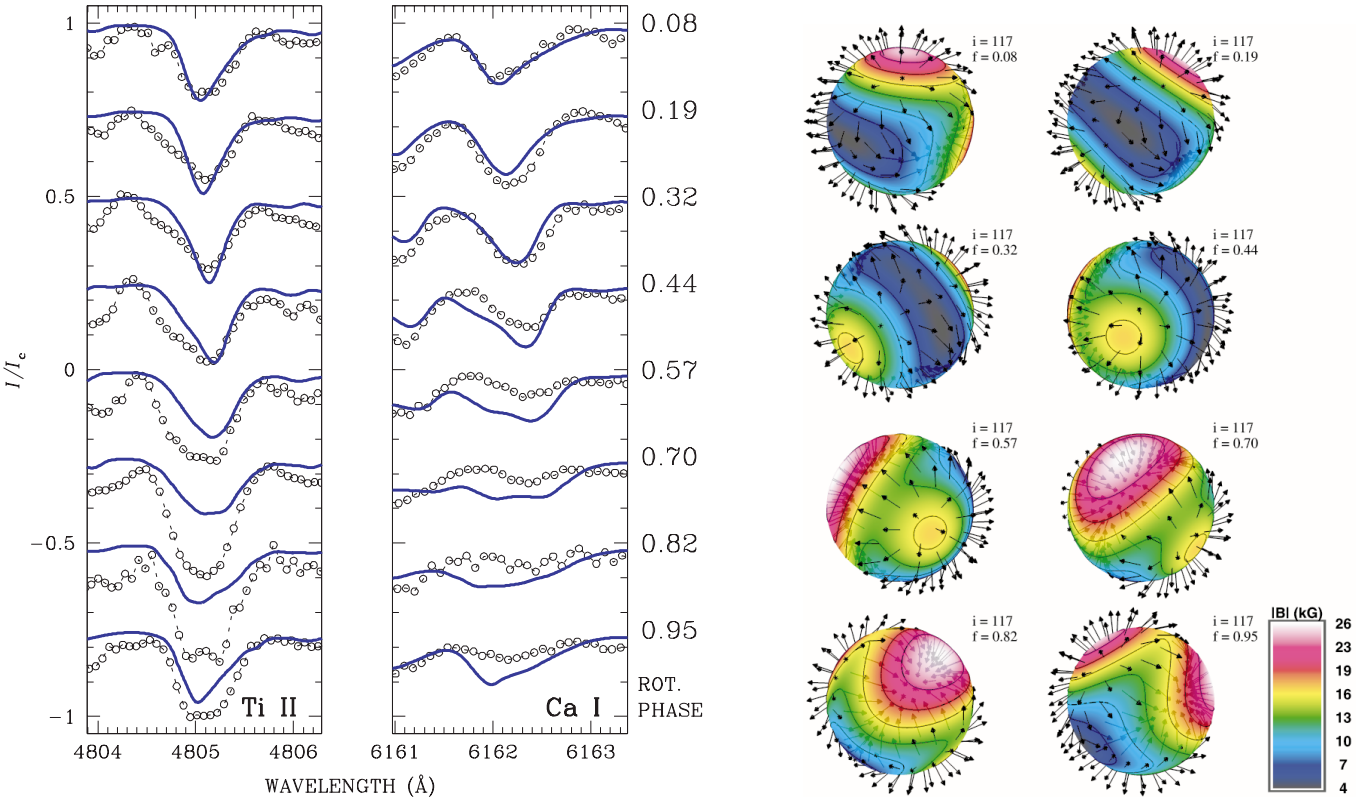

Fig. 9. 53 Cam. Left panels: the Ti II line at 4805.085 Å and the Ca I line at 6162.173 Å, compared to the model predictions assuming homogeneous distribution of the elements, given by [Ti/H] = 0.0 and [Ca/H] = +0.4, arbitrarily selected in order to account for the observations at phase = 0.08. Note that Ti I line is blended in the blue wing with a Fe II line, and in the red wing with a Cr I line, which leaves quite undetermined the real Ti abundance. Right panels: the model magnetic maps corresponding to the various rotation phases as the Stokes profiles shown in the left panels. Compare also with the magnetic curves of Fig. 7. The maximum of the longitudinal field curve occurs around phase 0.23. To a variance with axisymmetric models, no positive pole is in fact associated to this rotation phase

be recalled that the magnetic model depicted in Fig. 9 is not sufficient to explain the observed spectropolarimetric features of 53 Cam, and this example should rather serve to point out the need for more sophisticated modelling in order to provide guidance to diffusion theory.

For both β CrB and 53 Cam there is evidence for a strong vertical nonuniformity of the abundances of many elements, a phenomenon which has not been investigated in detail in this work. It is clear that if the magnetic field affects the element distribution, we should predict stratification effects which depend upon the magnetic topology, and hence which may also vary as the star rotates. Further work could be aimed at investigating whether such stratification variability is detectable.

8. Reliability of stellar magnetic field models

This investigation shows the limitations of the multipolar magnetic field models for β CrB and 53 Cam. Do these results affect the general reliability of the modelling technique itself? Although this investigation has involved a sample of only two objects, it would probably be naîve to believe that a similar analysis of other stars would lead to significantly more successful results. Therefore such a question is of very general interest, concerning both previous results and future researches on CP stars. On the one hand, our present knowledge of the magnetic fields of CP stars is just based on a more or less refined analysis of the magnetic observables; on the other hand, assessing the reliability of the modelling of the magnetic observables is of primary importance in order to address future observational and modelling efforts.

To address this problem it should first be pointed out that for both stars, discrepancies exist between model predictions and observations not only for the Stokes profiles, but also for the magnetic curves. This suggests that an intrinsic limit to the modelling technique lies in the assumption of a second-order multipolar expansion, and that a more sophisticated framework for the modelling is required (e.g., adding an octupolar component to describe the magnetic field). Accordingly, the results of this work do not discourage the use of the magnetic observables for deriving a tentative field model, although it is certainly worthwhile to explore alternative strategies. Further work is in progress, aimed at clarifying which strategy is most appropriate. Bagnulo, Mathys & Stift (in preparation) are performing numerical tests aimed at establishing the intrinsic accuracy of the determination of the magnetic observables from the low order moments of Stokes profiles; in

other words, how precise is the determination of the magnetic observables through the analysis of the low-order moments of Stokes profiles? Preliminary results confirm the accuracy of such a *moment technique*. Bagnulo & Wade (2001) are exploring the advantages of a direct inversion of Stokes profiles based on a multipolar expansion of the magnetic field. Other research groups are currently refining ZDI, either using a very specific regularisation function (in the form of a low order multipolar expansion; Kochukhov 2000; Piskunov 2001) or imposing physical constraints on the large scale field structure (e.g., that the field is potential or linear force-free; Donati 2001), in order to allow ZDI be effective for organised fields, even without Stokes Q and U observations. For the time being, we are left with the problem to evaluate the reliability of the presently available magnetic models of CP stars. What information do such models, which we conclude are oversimplified representations of the real field structure, really contain?

A recent statistical work carried out by Landstreet & Mathys (2000) has shown that slow rotators ($P \gtrsim 25\,\mathrm{d}$) have a magnetic field commonly characterised by an axisymmetric component nearly parallel to the rotation axis. Such a feature is so prominent so as to be correctly identified regardless our capability to explain the details of Stokes profiles. Other studies (Bagnulo et al. 1999b; Bagnulo & Landolfi 1999) exclude such a predominantly axisymmetric nature for faster rotators, showing in many cases evidence for a global field structure more complex than a second-order multipolar expansion. However, caution is needed for the interpretation of more detailed modelling results, as it is not clear how closely a model obtained with an insufficient number of free parameters may resemble to the real magnetic configuration.

An additional complication that we have not considered is a possible vertical structure of the magnetic field. The hypothesis of a topology which changes with optical depth was considered e.g. by Wolff (1978); Romanyuk (1986); Leroy (1995b). For β CrB and 53 Cam, inspection to Stokes profiles of different lines – probing different layers of the photospheres, do not show evidence for remarkable changes of the magnetic field with optical depth, yet, on the basis of our study, such a complex scenario *cannot* firmly be rule out. However, it should be noted that although of complex topology, the magnetic field at the surface of CP stars varies on a large scale, typically $\gg 10^5$ km. This makes it hard to expect a substantial variation of the magnetic structure along the vertical dimension of the photosphere, which is only a few thousand km in depth.

9. Conclusions

We have attempted to reproduce the observed Stokes $IQUV$ profiles of two well known magnetic stars: β CrB and 53 Cam. For this purpose, we have started with a well established technique for modelling the *magnetic observables* (see Sect. 1), resulting in constraints to the magnetic geometry (Mathys 1999; Landolfi et al. 1998; Bagnulo et al. 2000). The candidate magnetic models obtained with this technique have then been used as input to a spectral synthesis code, and the theoretical Stokes profiles have subsequently been compared to new spectropolarimetric observations of the two stars in question.

For β CrB we have limited ourselves to a comparison of spectropolarimetric observations with two magnetic models previously presented in the literature (Bagnulo et al. 2000). For 53 Cam, we have used an axisymmetric model proposed by Landstreet (1988), and we have attempted to find a more adequate, non axisymmetric magnetic model.

The results for β CrB show that none of the models suggested by Bagnulo et al. (2000) is sufficient to account fully for the polarization features at all observed rotational phases. No obvious evidence is found in Stokes I for a horizontal inhomogeneity of the element abundances, although the stellar geometry view is such that, if such inhomogeneities exist, they would hardly be detectable (in Stokes I), as they are more or less permanently visible on the stellar disk. A striking inconsistency was found when we attempted to reproduce both weak and strong spectral lines of a given ion, with unique value for the element abundance, a phenomenon which is likely due to chemical stratification (Babel & Lanz 1992), involving virtually all ions identified in the stellar spectrum.

The comparison of synthetic vs. observed Stokes profiles for 53 Cam yields even poorer agreement than for β CrB, as all models largely overestimate the amplitude of the observed linear polarization. Keeping in mind that the linear polarization characteristics of spectral lines are more sensitive to the magnetic orientation than those of the circular polarization or of the unpolarized part of the radiation, this finding suggests a scenario where the magnetic field of 53 Cam is considerably more complex than can be described by a second order multipolar expansion. In such a complex topology, the contributions to the linearly polarized radiation of spectral lines coming from different parts of the stellar surface will tend to cancel. Such complex fields may also be characteristic of the majority of (cool) CP stars for which Leroy (1995a) failed to detect a conspicuous BBLP signal. Both Ti II and Ca I are found to exhibit clear horizontally nonuniformities across the stellar surface, but no firm conclusion was obtained regarding the relationship between magnetic topology and geographic variation of these elements. Evidence for stratification is again found for virtually all identified ions.

We finish by pointing out a general conclusion of this work. Any realistic study of the photopheres of magnetic CP stars must consider the atmosphere as a three dimensional structure permeated by a complex magnetic field, taking into account not only horizontal nonuniformities of chemical abundances, but also their important vertical variations as well. This implies that we need more accurate model atmospheres, accounting for element stratification and magnetic force, and more sophisticated modelling techniques for stellar magnetic fields.

Acknowledgements. S. Bagnulo and M. J. Stift gratefully acknowledge financial support by the Austrian *Fonds zur Förderung der Wissenschaftlichen Forschung*, project P12101-AST. SB thanks also the hospitality of the Department of Physics and Astronomy of UWO. This work has been funded in part by the Natural Science and Engineering Research Council of Canada. We thank G. G. Valyavin for his help to obtain the observations of 53 Cam at SAO.

References

Adelman, S. J. 1985, PASP, 97, 970
Auer, L. H., Heasley, J. N., & House, L. L. 1977, ApJ, 216, 531
Babcock, H. W. 1947, ApJ, 105, 105
Babcock, H. W. 1958, ApJS, 3, 141
Babcock, H. W. 1960a, ApJ, 132, 521
Babcock, H. W. 1960b, in Stellar Atmospheres, ed. J. Greenstein (University of Chicago Press, Chicago), 282
Babel, J. 1992, A&A, 258, 449
Babel, J. 1994, A&A, 283, 189
Babel, J., & Lanz, T. 1992, A&A, 263, 232
Babel, J., & Michaud, G. 1992, ApJ, 366, 560
Bagnulo, S., Landi Degl'Innocenti, E., Landolfi, M., & Leroy, J.-L. 1995, A&A, 295, 459
Bagnulo, S., Landi Degl'Innocenti, M., & Landi Degl'Innocenti, E. 1996, A&A, 308, 115
Bagnulo, S., & Landolfi, M. 1999, A&A, 346, 158
Bagnulo, S., Stift, M. J., Leone, F., Kurtz, D. W., & Martinez, P. 1999a, in Solar Polarization, ed. K. N. Nagendra, & J. O. Stenflo (Kluwer, Dordrecht), 459
Bagnulo, S., Landolfi, M., & Landi Degl'Innocenti, M. 1999b, A&A, 343, 865
Bagnulo, S., & Wade, G. 2001, in Proceedings of the Workshop "Magnetic Fields across the Hertzsprung-Russell Diagram", A.S.P. Conf. Ser., ed. G. Mathys, S. K. Solanki, & D. T. Wickramasinghe, in press
Bagnulo, S., Landolfi, M., Mathys, G., & Landi Degl'Innocenti, M. 2000, A&A, 358, 929
Baudrand, J., & Böhm, T. 1992, A&A, 259, 711
Borra, E. F. 1974, ApJ, 188, 287
Borra, E. F., & Landstreet, J. D. 1973, ApJ, 185, L139
Borra, E. F., & Landstreet, J. D. 1977, ApJ, 212, 141
Borra, E. F., & Landstreet, J. D. 1980, ApJS, 42, 421
Borra, E. F., & Vaughan, A. H. 1977, ApJ, 216, 478
Brillant, S., Stehlé, C., & Mathys, G. 1999, in Solar Polarization, ed. K. N. Nagendra, & J. O. Stenflo (Kluwer, Dordrecht), 479
Brown, S. F., Donati, J.-F., Rees, D. E., & Semel, M. 1991, A&A, 250, 463
Calamai, G., Landi Degl'Innocenti, E., & Landi Degl'Innocenti, M. 1975, A&A, 45, 287
Donati, J.-F., 2000, in First International Workshop on Astro-Tomography, ed. H. Boffin, D. Steeghs, & J. Cuypers, in press
Donati, J.-F., Semel, M., & del Toro Iniestia, J. C. 1990, A&A, 233, L17
Donati, J.-F., & Brown, S. F. 1997, A&A, 326, 1135
Donati, J.-F., Semel, M., Carter, B. D., Rees, D. E., & Cameron, A. C. 1997, MNRAS, 291, 658
Donati, J.-F., Cameron, A. C., Hussain, G. A. J., & Semel, M. 1999a, MNRAS, 302, 437
Donati, J.-F., Catala C., Wade G. A., et al. 1999b, A&AS, 134, 149
Faraggiana, R., & Gerbaldi, M. 1993, in Peculiar versus normal phenomena in A-type and related stars, I.A.U. Colloquium No. 138, ed. M. M. Dworetsky, F. Castelli, & R. Faraggiana, ASP Conf. Ser., 44, 169
Fensl, R. M. 1995, A&AS, 112, 191
Grevesse, N., & Anders, E. 1991, in Solar interior and atmosphere, Tucson, AZ (University of Arizona Press), 1227
Hauck, B., & North, P. 1982, A&A, 114, 23
Hauck, B., & North, P. 1993, A&A, 269, 403
Hildebrandt, G., Scholz, G., & Woche, M. 1997, Astron. Nachr., 318, 291
Hill, G. M., Bohlender, D. A., Landstreet, J. D., et al. 1998, MNRAS, 297, 236
Hubrig, S., North, P., & Mathys, G. 2000, ApJ, 539, 352
Huchra, J. 1972, ApJ, 174, 435
Kemp, J. C., & Wolstencroft, R. D. 1974, MNRAS, 166, 1
Kochukhov, O. P. 2000, in Proceedings of Stellar Magnetic Fields, Special Astrophysical Observatory, Moskow, 106
Landi Degl'Innocenti, M., Calamai, G., Landi Degl'Innocenti, E., & Patriarchi, P. 1981, ApJ, 249, 228
Landolfi, M., & Landi Degl'Innocenti, E. 1982, Solar Phys., 78, 355
Landolfi, M., Landi Degl'Innocenti, E., Landi Degl'Innocenti, M., & Leroy, J.-L. 1993, A&A, 272, 285
Landolfi, M., Bagnulo, S., & Landi Degl'Innocenti, M. 1998, A&A, 338, 111
Landstreet, J. D. 1988, ApJ, 326, 967
Landstreet, J. D. 1992, A&AR, 4, 35
Landstreet, J. D., & Mathys, G. 2000, A&A, 359, 213
Landstreet, J. D., Barker, P. K., Bohlender, D. A., & Jewison, M. S. 1989, ApJ, 344, 876
Leone, F., & Manfrè, M. 1997, A&A, 320, 257
Leone, F., Catanzaro, G., & Catalano, S. 2000, A&A, 355, 315
Leone F., & Catanzaro, G. 2001, A&A, 365, 118
Leroy, J.-L. 1962, Ann. Astrophys., 25, 127
Leroy J.-L. 1990, A&A, 237, 237
Leroy, J.-L. 1995a, A&AS, 114, 79
Leroy, J.-L. 1995b, in La Polarimétrie, outil pour l'étude de l'activité magnétique solaire et stellaire, ed. N. Mein, & S. Sahal-Bréchot, Observatoire de Paris
Leroy, J.-L., Landolfi, M., & Landi Degl'Innocenti, E. 1996, A&A, 311, 513
Martin, C., & Mignard, F. 1998, A&AS, 330, 585
Mathys, G. 1989, Fundamentals of Cosmic Physics, 113, 143
Mathys, G. 1991, A&AS, 89, 121
Mathys, G. 1995a, A&A, 293, 733
Mathys, G. 1995b, A&A, 293, 746
Mathys, G. 1999, in Solar Polarization, ed. K. N. Nagendra, & J. O. Stenflo (Kluwer, Dordrecht), 489
Mathys, G., Hubrig, S., Landstreet, J. D., Lanz, T., & Manfroid, J. 1997, A&AS, 123, 353
Mathys, G., Stehlé, C., Brillant, S., & Lanz, T. 2000, A&A, 358, 1151
Michaud, G. 1970, ApJ, 160, 641
Moss, D. 1994, in Pulsation, rotation, and mass loss in early-type stars, I.A.U. Symposium No. 162, ed. L. A. Balona, H. F. Henrichs, & J. M. Contel (Kluwer Academic Publishers, Dordrecht), 173
Musaev, F. A. 1996, Astron. Lett., 22, 715
Musielok, B., & Madej, J. 1988, A&A, 202, 143.
Piskunov, N. E. 1999, in Solar Polarization, ed. K. N. Nagendra, & J. O. Stenflo (Kluwer, Dordrecht), 515

Piskunov, N. E. 2001, in First International Workshop on Astro-Tomography, ed. H. Boffin, D. Steeghs, & J. Cuypers, in press
Piskunov, N. E., Kupka, F., Ryabchikova, T. A., Weiss, W. W., & Jeffery, C. S. 1995, A&AS, 112, 525
Preston, G. W., & Stępień, K. 1968, ApJ, 151, 583
Preston, G. W. 1969, ApJ, 157, 247
Romanyuk, I. I. 1986, in Upper Main Sequence Stars with Anomalous Abundances, ed. R. Cowley, M. Dworetsky, & M. Megessier (Dordrecht, D. Reidel Publishing Co.), ASSL series vol. 125, 359
Rees, D. E., Murphy, G. A., & Durrant, C. J. 1989, ApJ, 339, 1093
Savanov, I. S., & Kochukhov, O. P. 1998, Astron. Lett., 24, 601
Semel, M. 1989, A&A, 225, 456
Semel, M., Donati, J.-F., & Rees, D. E. 1993, A&A, 278, 231
Scholz, G., & Lehmann, H. 1988, Astron. Nachr., 309, 33
Shurcliff, W. A. 1962, Polarized light (Harvard University Press, Cambridge)
Stępień, K. 2000, A&A, 353, 227
Stibbs, D. W. N. 1950, MNRAS, 110, 395
Stift, M. J. 1975, MNRAS, 172, 133
Stift, M. J. 1985, MNRAS, 217, 55
Stift, M. J. 1998, in Solar Polarization, ed. K. N. Nagendra, & J. O. Stenflo (Kluwer, Dordrecht), 241
Stift, M. J. 2000, A Peculiar Newsletter, 34
Stift, M. J., & Goossens, M. 1991, A&A, 251, 139
Wade, G. A., Donati, J.-F., Landstreet, J. D., & Shorlin, S. L. S. 2000a, MNRAS, 313, 823
Wade, G. A., Donati, J.-F., & Landstreet, J. D. 2000b, New Astron. 5, 455
Wade, G. A., Donati, J.-F., Landstreet, J. D., & Shorlin, S. L. S. 2000c, MNRAS, 313, 851
Wolff, S. C. 1978, PASP, 90, 412
Wolff, S. C., & Wolff, R. J. 1970, ApJ, 160, 1049